

## ADAPTATION AND TRANSMITTER GATING IN VERTEBRATE PHOTORECEPTORS

GAIL A. CARPENTER\*

*Department of Mathematics, Northeastern University,  
Boston, MA 02115, U.S.A.*

and

STEPHEN GROSSBERG\*\*

*Department of Mathematics, Boston University,  
Boston, MA 02215, U.S.A.*

(Received February 12, 1981)

### Abstract

A quantitative model for the transduction dynamics whereby intracellular transmitter in a vertebrate cone mediates between light input and voltage output is analyzed. A basic postulate is that the transmitter acts to multiplicatively gate the effects of light before the gated signal ever influences the cone potential. This postulate does not appear in the Baylor, Hodgkin, and Lamb (BHL) model of cone dynamics. One consequence of this difference is that a single dynamic equation from our model can quantitatively fit turtle cone data better than the full BHL theory. The gating concept also permits conceptually simple explanations of many phenomena whose explanations using the BHL unblocking concept are much more complex. Predictions are suggested to further distinguish the two theories.

Our transmitter laws also form a minimal model for an unbiased miniaturized transduction scheme which can be realized by a depletable transmitter. Thus our theory allows us to consider more general issues. Can one find an optimal transmitter design of which the photoreceptor transmitter is a special case? Does the cone transmitter obey laws that are shared by transmitters in other neural systems, with which the photoreceptors can be compared and contrasted to distinguish its specialized design features from its generally shared features?

### 1. Introduction

Abundant experimental evidence has shown that many vertebrate photoreceptors undergo large sensitivity changes during light and dark adaptation, and that receptor adaptation is a significant component of the adaptive process (Boynton and Whitten, 1970; Dowling and Ripps, 1971, 1972; Grabowski *et al.*, 1972; Kleinschmidt, 1973; Kleinschmidt and Dowling, 1975; Norman and Werblin, 1974). Various studies also suggest that light liberates internal transmitter mole-

\* Supported in part by National Science Foundation (MCS-80-04021) and the Northeastern University Research and Scholarship Development Fund.

\*\* Supported in part by the National Science Foundation (NSF IST-80-00257).

GAIL A. CARPENTER AND STEPHEN GROSSBERG

cles, possibly of  $\text{Ca}^{++}$ , which close  $\text{Na}^+$  channels in the plasma membrane of the photoreceptor outer segment, thereby decreasing the 'dark current' of  $\text{Na}^+$  ions entering this membrane and hyperpolarizing the photoreceptor (Arden and Low, 1978; Bäckström and Hemilä, 1979). Extensive parametric experiments on turtle cones have shown the adaptive process to be highly nonlinear (Baylor and Hodgkin, 1974; Baylor *et al.*, 1974*a,b*). From these data, Baylor *et al.* (1974*b*) constructed an ingenious model of cone dynamics which quantitatively reproduces many data features. However, the model's voltage reactions are a factor of ten off in response to flashes on variable backgrounds and, more importantly, the timing of voltage peaks does not fit the data well. Other quantitative difficulties can also be cited.

We will suggest that the quantitative difficulties of the BHL model are also qualitative, and are due to the model's omission of a major feature of cone design. The BHL model omits the basic postulate that the transmitter acts to multiplicatively gate the effects of light before the gated signal ever influences the cone potential. Without the notion of a multiplicative transmitter gate, the full BHL theory grew in a different direction than our own.

We have achieved a better quantitative fit of the BHL data using a transmitter model that was introduced in 1968 (Grossberg, 1968, 1969). In fact, for key experiments we achieve a better quantitative fit using a single dynamic equation from our theory than BHL do with their full theory with many equations. These successes can be traced to the inclusion within our theory of a multiplicative transmitter gate.

Our goal in this article is not merely to use this transmitter model to fit photoreceptor data. We wish also to make a general point concerning neural modelling. The BHL model, despite its many partial successes, is in a sense profoundly disturbing. It leaves one with the impression that the photoreceptor is not merely complex, but also that its complexities describe a rather mysterious transduction scheme with properties that seem impossible to guess *a priori*. If this is the true situation at each photoreceptor, then what hopes can we sustain for finding understandable principles of neural organization in the large?

We will derive our transmitter laws as a minimal model for an unbiased miniaturized transduction scheme that can be realized by a depletable chemical (Grossberg, 1980). Because the principles from which these laws are derived have a general significance, our theory allows us to suggest affirmative answers to the following more general questions: Can one find an optimal transmitter design of which the photoreceptor is a special case? Does the cone transmitter obey laws that are shared by transmitters in other neural systems, with which the photoreceptor can be compared and contrasted to distinguish its specialized design features from its generally shared features?

A gating concept appears in the model of Hemilä (1977, 1978), which Hemilä used to explain adaptation in the rods of the frog retina. Hemilä does not, however, suggest dynamical laws for the gating process. Both the BHL theory and our theory suggest that transmitter can close  $\text{Na}^+$  channels. BHL call this process

‘blocking’. It is at this point that the two theories diverge. The BHL theory invokes a process to ‘unblock’ the blocking process. We never need such an idea. Once the unblocking concept is accepted, however, it naturally suggests a series of auxiliary hypotheses which diverge significantly from the ideas that emerge from a gating concept.

Our theory also explains photoreceptor data from systems other than turtle cones, such as data from *Gekko gekko* rods (Kleinschmidt and Dowling, 1975). Because gating mechanisms are also used in nonvisual transmitter systems, adaptation, overshoot and rebound of the rod potential can be compared and contrasted with analogous phenomena in midbrain reinforcement centers (Grossberg 1972*a,b*, 1981*a,b*). The *Gekko gekko* data can, for example, be explained by a *gated dipole* model which shows how slow gates acting on the signals within competing channels can elicit adaptation, overshoot and rebound. In the rod, the dipole is due to intracellular membrane interactions; in the midbrain, it is due to intercellular network interactions. This type of insight would be impossible to achieve were our theory not derived from a general principle of neural design.

In Sections 2–13 of this article we derive the gating theory and its predictions. In Section 14 we fit the theory to photoreceptor data. In Sections 14–15 we contrast the gating theory with BHL’s unblocking theory.

## 2. Transmitters as gates

We start by asking the following question: What is the simplest law whereby one nerve cell could conceivably send unbiased signals to another nerve cell? The simplest law says that if a signal  $S$  passes through a given nerve cell  $v_1$ , the signal  $S$  has a proportional effect

$$(1) \quad T = SB$$

where  $B > 0$ , on the next nerve cell  $v_2$ . Such a law would permit unbiased transmission of signals from one cell to another.

We are faced with a dilemma, however, if the signal from  $v_1$  to  $v_2$  is due to the release of a chemical  $z(t)$  from  $v_1$  that activates  $v_2$ . If such a chemical transmitter is persistently released when  $S$  is large, what keeps the net signal  $T$  from getting smaller and smaller as  $v_1$  runs out of transmitter? Some means of replenishing, or accumulating, the transmitter must exist to counterbalance its depletion due to release from  $v_1$ .

Based on this discussion, we can rewrite (1) in the form

$$(2) \quad T = Sz$$

and ask how the system can keep  $z$  replenished so that

$$(3) \quad z(t) \cong B$$

at all times  $t$ . This is a question about the *sensitivity* of  $v_2$  to signals from  $v_1$ , since if  $z$  could decrease to very small values, even large signals  $S$  would have only a small effect on  $T$ .

Equation (2) has the following interpretation. The signal  $S$  causes the transmitter  $z$  to be released at a rate  $T = Sz$ . Whenever two processes, such as  $S$  and  $z$ , are multiplied, we say that they interact by *mass action*, or that  $z$  *gates*  $S$ . Thus (2) says that  $z$  gates  $S$  to release a net signal  $T$ , and (3) says that the cell tries to replenish  $z$  to maintain the system's sensitivity to  $S$ . Data concerning the gating action of transmitters in several neural preparations have been collected by Čapek *et al.* (1971), Esplin and Zablocka-Esplin (1971), Zablocka-Esplin and Esplin (1971).

What is the simplest law that joins together both (2) and (3)? It is the following differential equation for the net rate of change  $dz/dt$  of  $z$ :

$$(4) \quad \frac{dz}{dt} = A(B - z) - Sz.$$

Equation (4) describes the following four processes going on simultaneously.

#### *I and II. Accumulation and Production and feedback inhibition.*

The term  $A(B - z)$  enjoys two possible interpretations, depending on whether it represents a passive accumulation process or an active production process.

In the former interpretation, there exist  $B$  sites to which transmitter can be bound,  $z$  sites are bound at time  $t$ , and  $B - z$  sites are unbound. Then term  $A(B - z)$  says simply that transmitter is bound at a rate proportional to the number of unbound sites.

In the latter interpretation, two processes go on simultaneously. Term  $AB$  on the righthand side of (4) says that  $z$  is produced at a rate  $AB$ . Term  $-Az$  says that once  $z$  is produced, it inhibits the production rate by an amount proportional to  $z$ 's concentration. In biochemistry, such an inhibitory effect is called *feedback inhibition* by the end product of a reaction. Without feedback inhibition, the constant rate  $AB$  of production would eventually cause the cell to burst. With feedback inhibition, the net production rate is  $A(B - z)$ , which causes  $z(t)$  to approach the finite amount  $B$ , as we desire by (3). The term  $A(B - z)$  thus enables the cell to accumulate a target level  $B$  of transmitter.

#### *III and IV. Gating and Release.*

Term  $-Sz$  in (4) says that  $z$  is released at a rate  $Sz$ , as we desire by (2). As in (2), release of  $z$  is due to mass action activation of  $z$  by  $S$ , or to gating of  $S$  by  $z$  (Figure 1).

The two equations (2) and (4) describe the simplest dynamic law that 'corresponds' to the constraints (2) and (3). Equations (2) and (4) hereby begin to reconcile the two constraints of unbiased signal transmission and maintenance of sensitivity when the signals are due to release of transmitter. All later refinements of the theory describe variations on this robust design theme.

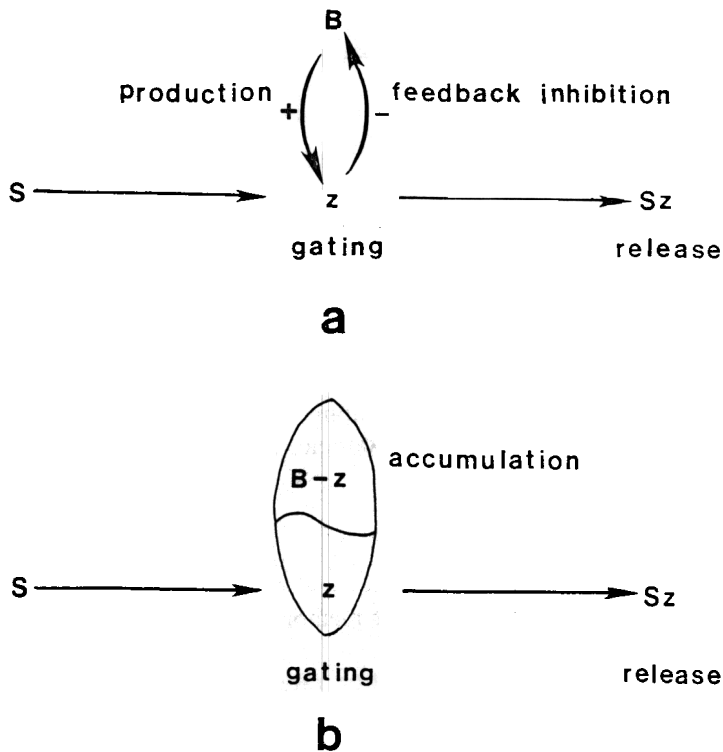


Fig. 1. (a) Production, feedback inhibition, gating and release of a transmitter  $z$  by a signal  $S$ . (b) Mass action transmitter accumulation at unoccupied sites has the same formal properties as production and feedback inhibition.

### 3. Intracellular adaptation and overshoot

Before describing these variations, let us first note that Equations (2) and (4) already imply important qualitative features of photoreceptor dynamics; namely, adaptation to maintained signal levels, and overshoot in response to sudden changes of signal level.

Suppose for definiteness that  $S(t) = S_0$  for all times  $t \leq t_0$  and that at time  $t = t_0$ ,  $S(t)$  suddenly increases to  $S_1$ . By (4),  $z(t)$  reacts to the constant level  $S(t) = S_0$  by approaching an equilibrium value  $z_0$ . This equilibrium value is found by setting  $dz/dt = 0$  in (4) and solving to get

$$(5) \quad z_0 = \frac{AB}{A + S_0}.$$

By (2), the net signal  $T_0$  to  $v_2$  at time  $t = t_0$  is

$$(6) \quad S_0 z_0 = \frac{ABS_0}{A + S_0}.$$



Now let  $S(t)$  switch to the value  $S_1 > S_0$ . Because  $z(t)$  is slowly varying,  $z(t)$  approximately equals  $z_0$  for some time after  $t = t_0$ . Thus the net signal to  $v_2$  during these times is approximately equal to

$$(7) \quad S_1 z_0 = \frac{ABS_1}{A + S_0}.$$

Equation (7) has the same form as a Weber law  $J(A + I)^{-1}$ . The signal  $S_1$  is evaluated relative to the baseline  $S_0$  just as  $J$  is evaluated relative to  $I$ . The Weber law in (7) is due to slow intracellular adaptation of the transmitter to the sustained signal level. A Weber law can also be caused by fast intercellular lateral inhibition across space, but the mechanisms underlying these two adaptive processes are entirely different (Grossberg 1973, 1980).

The capability for intracellular adaptation can be destroyed by matching the reaction rate of the transmitter to the fluctuation rate in  $S(t)$ . For example, if  $z(t)$  reacts as quickly as  $S(t)$ , then at all times  $t$ ,

$$(8) \quad T(t) \cong \frac{ABS(t)}{A + S(t)}$$

no matter what values  $S(t)$  attains, so that the adaptational baseline, or memory of prior input levels, is destroyed.

A basis for overshoot behavior can also be traced to  $z$ 's slow reaction rate. If  $z(t)$  in (4) reacts slowly to the new transmitter level  $S = S_1$ , it gradually approaches the new equilibrium point that is determined by  $S = S_1$ , namely

$$(9) \quad z_1 = \frac{AB}{A + S_1}$$

as the net signal decays to the asymptote

$$(10) \quad S_1 z_1 = \frac{ABS_1}{A + S_1}$$

Thus after  $S(t)$  switches from  $S_0$  to  $S_1$ , the net signal  $T = Sz$  jumps from (6) to (7) and then gradually decays to (10) (Figure 2). The exact course of this overshoot and decay is described by the equation

$$(11) \quad S_1 z(t) = \frac{ABS_1}{A + S_0} \exp\{-(A + S_1)(t - t_0)\} + \frac{ABS_1}{A + S_1} (1 - \exp\{-(A + S_1)(t - t_0)\})$$

followed by slow decay of  $T$  is called 'overshoot' in a photoreceptor and 'habituation' in various other neural preparations.

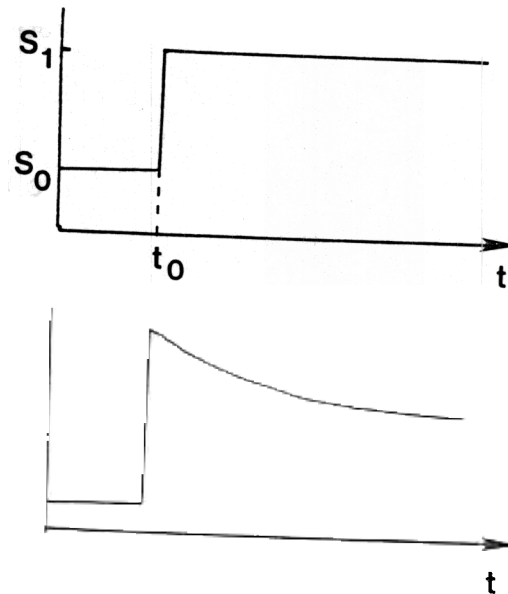


Fig. 2. Overshoot and habituation of the gated signal  $T = Sz$  due to a sudden increment in signal  $S$ .

#### 4. Monotonic increments and nonmonotonic overshoots to flashes on variable backgrounds

The minimal transmitter model implies more subtle properties as well. Some of these properties figure prominently in our explanation of the BHL data. Others stand as experimental predictions. Baylor *et al.* (1974b) found that, in response to a flash of fixed size superimposed on a succession of increasing background intensities, the cone potential  $V$  reacts with a progressive decrease in the size of its transient response. By contrast,  $V$ 's transient response reaches its peak at successively earlier times until a sufficiently high background intensity is reached. In response to even higher background intensities, the potential reaches its peak at successively later times (Figure 3). This is a highly nonlinear effect.

In our theory,  $T$  is the input to the photoreceptor's potential  $V$ . We study  $T$  in its own right to provide a better understanding of  $V$ 's behavior in the full theory. Simple approximations make possible analytic estimates that qualitatively explain the behavior in Figure 3. Since a flash sets off a chain reaction in the cone, and the chain reaction lasts for some time after the flash terminates, we approximate the chain reaction by a rectangular step of fixed size  $\delta$ . When a flash occurs at a succession of background intensities, we superimpose the step  $\delta$  on a succession of background intensities  $S$  (Figure 4). We estimate the effect of the flash on

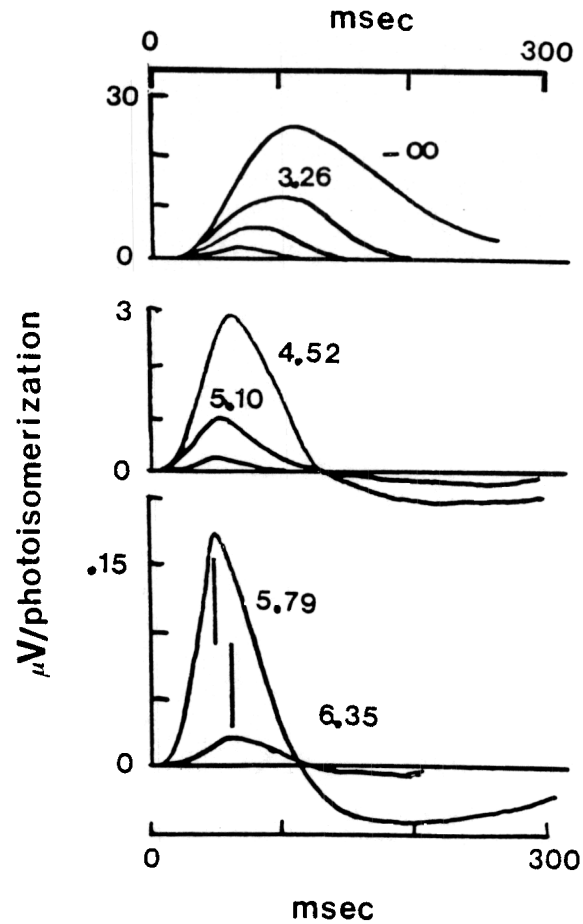


Fig. 3. The transient reactions of a cone potential to a fixed flash superimposed on a succession of increasing background levels. The potential peaks decrease, whereas the times of maximal potential first decrease and then increase, as the background parametrically increases. Effect of increasing intensity of conditioning step on response to 11 msec flash applied 1.1 sec after beginning of a step lasting 1.7 sec. The abscissa is the time after the middle of the flash, and the ordinate is  $U(t)/I\Delta t$ , where  $U(t)$  is the hyperpolarization,  $\Delta t$  is the pulse duration, and  $I$  is proportional to flash intensity. The numbers against the curves give the logarithm of the conditioning light expressed in photoisomerizations  $\text{cone}^{-1} \text{sec}^{-1}$ . Redrawn from Fig. 3 (Baylor and Hodgkin 1974), p. 734.

the potential peak by computing the initial change in  $T$  due to the change in  $S$  by  $\delta$ . We also estimate a possible initial 'hump' in the potential through time by measuring the height and the area of the overshoot created by prescribed background levels  $S$  (Figure 4).

The initial change in  $T$  to a change in  $S$  by  $\delta$  is found to be a decreasing function

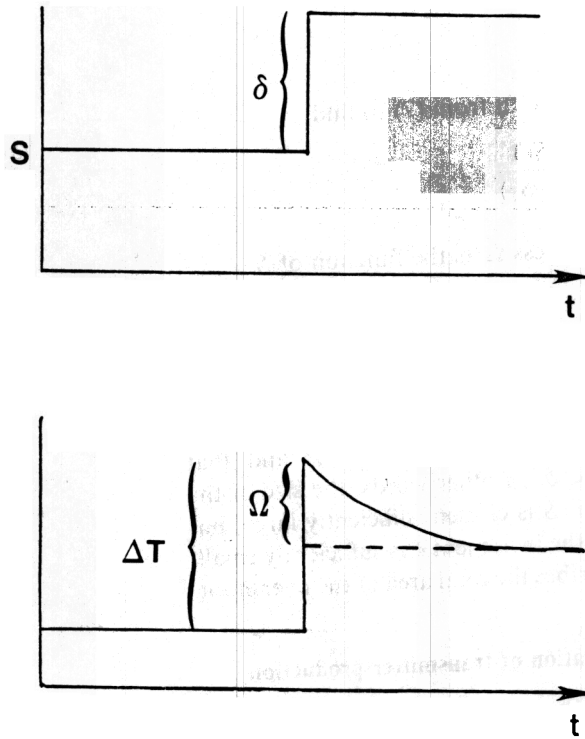


Fig. 4. An input step of fixed size  $\delta$  on a background  $S$  causes a transient change in  $T$  of size  $\Delta T$  and an overshoot of size  $\Omega$ .

of  $S$ . This result is analogous to the decreasing size of the potential change caused by a fixed flash at successively higher background intensities. However, the size of the overshoot, or 'hump', need not be a decreasing function of  $\delta$ . If  $\delta$  is sufficiently small, then the overshoot size can increase before it decreases as a function of  $\delta$ . In other words, a more noticeable hump can appear at large background intensities  $S$ , but it can eventually shrink as the background intensity is increased even further. Baylor *et al.* (1974b) report humps at high background intensities as well as their shrinkage at very high background intensities.

To estimate the change  $\Delta T$  due to a step size of  $\delta$ , we subtract (6) from (7) to find

$$(12) \quad \Delta T = \frac{AB(S_1 - S_0)}{A + S_0}$$

Let  $S_1 - S_0 = \delta$ , corresponding to a step of fixed size  $\delta$  superimposed after  $S(t)$  equilibrates to a background intensity  $S_0 = S$ . Then

$$(13) \quad \Delta T = \frac{AB\delta}{A + S}$$

which is a decreasing function of  $S$ .

To estimate the overshoot size  $\Omega$ , we subtract (10) from (7) to find

$$(14) \quad \Omega = \frac{ABS_1(S_1 - S_0)}{(A + S_0)(A + S_1)}$$

Again setting  $S_1 - S_0 = \delta$  and  $S_0 = S$ , we express  $\Omega$  as the function of  $S$

$$(15) \quad \Omega(S) = \frac{AB(S + \delta)\delta}{(A + S)(A + S + \delta)}$$

How does  $\Omega(S)$  change as a function of  $S$ ? To test whether  $\Omega(S)$  increases or decreases as a function of  $S$ , we compute whether  $d\Omega/dS$  is positive or negative. One readily proves that  $d\Omega/dS > 0$  at  $S = 0$  if  $A > \frac{1}{2}(1 + \sqrt{5})\delta$ ; and that  $d\Omega/dS < 0$  if  $S > -\delta + \sqrt{A(A - \delta)}$  or if  $A < \delta$ . In other words, the size of the overshoot always decreases as a function of  $S$  if  $S$  is chosen sufficiently large, but the overshoot size increases at small  $S$  values if the increment  $\delta$  is sufficiently small. A similar type of nonmonotonic behaviour describes the total area of the overshoot.

### 5. Miniaturized transducers and enzymatic activation of transmitter production

We will now discuss how the time at which the potential reaches its peak can first decrease and then increase as a function of background intensity. Our discussion again centers on the design theme of ensuring the transducer's sensitivity. By proceeding in this principled fashion, we can explain more than the 'turn-around' of the potential peaks. We can also explain why the steady-state of  $T$  as a function of  $S$  can obey a law of the form

$$(16) \quad T = \frac{PS(1 + QS)}{1 + RS + US^2}$$

with  $P$ ,  $Q$ ,  $R$  and  $U$  constants, rather than a law of the form

$$(17) \quad T = \frac{PS}{1 + RS}$$

as in (6).

Equation (16) is the analog within our theory of the BHL equation

$$(18) \quad \frac{z_1}{K} = \frac{PS(1 + QS)}{1 + RS}$$

for the steady-state level of their 'blocking' variable  $z_1$ . Equation (18) cannot be valid at very large  $S$  values because it predicts that  $z_1$  can become arbitrarily large, which is physically meaningless. This does not happen in (16). The appearance of

term  $US^2$  in (16) allows us to fit BHL's steady-state data better than they could using (18). More important than this quantitative detail is the qualitative fact that the mechanism which replaces (17) by (16) also causes the turn-around in the peak potential. We now suggest that this mechanism is a light-induced enzymatic modulation of transmitter production and/or mobilization rates. Thus we predict that selective poisoning of this enzymatic mechanism can simultaneously abolish the turn-around in the potential peak and reduce (16) to (17).

The need for enzymatic modulation can be motivated by the following considerations. Despite the transmitter accumulation term  $A(B - z)$  in Equation (4), habituation to a large signal  $S$  can substantially deplete  $z$ , as in (5). What compensatory mechanism can counteract this depletion as  $S$  increases? Can a mechanism be found that maintains the sensitivity of the transmitter gate even at large  $S$  values?

One possibility is to store an enormous amount of transmitter, just in case; that is, choose a huge constant  $B$  in (4). This strategy has the fatal flaw that a very large storage depot takes up a lot of space. If each photoreceptor is large, then the number of photoreceptors that can be packed into a unit retinal area will be small. Consequently the spatial resolution of the retina will be poor in order to make its resolution of individual input intensities good. This solution is unsatisfactory.

Given this insight, our design problem can be stated in a more refined fashion as follows: How can a *miniaturized* receptor maintain its sensitivity at large input values?

An answer is suggested by inspection of Equation (4). In Equation (4), the transmitter depletion rate  $-Sz$  increases as  $S$  increases, but the transmitter production rate  $A$  is constant. If the production rate keeps up with the depletion rate, then transmitter can be made continuously available even if  $B$  is not huge. The marriage of miniaturization to sensitivity hereby suggests that the coefficient  $A$  is enzymatically activated by the signal  $S$ .

Let us suppose that this enzymatic step obeys the simplest mass action equation.

$$(19) \quad \frac{dA}{dt} = -C(A - A_0) + D[E - (A - A_0)]S.$$

In (19),  $A(t)$  has a baseline level  $A_0$  in the dark ( $S = 0$ ). Turning light on makes  $S$  positive and drives  $A(t)$  towards its maximum value  $A_0 + E$ . Rewriting (19) as

$$(20) \quad \frac{dA}{dt} = -(C + DS)(A - A_0) + DES$$

shows that the activation of  $A(t)$  by a constant signal  $S$  increases the gain  $C + DS$  as well as the asymptote

$$(21) \quad A = A_0 + \frac{DES}{C + DS}$$

of  $A(t)$ . This asymptote can be rewritten in the convenient form

$$(22) \quad A = A_0 \left( \frac{1 + FS}{1 + GS} \right)$$

by using the notation

$$(23) \quad F = (A_0 + E)DA_0^{-1}C^{-1}$$

and

$$(24) \quad G = DC^{-1}.$$

To make our main qualitative points, let us assume for the moment that the enzymatic activation of  $A$  by  $S$  proceeds much more rapidly than the release of  $z$  by  $S$ . Then  $A(t)$  approximately equals its asymptote in (22) at all times  $t$ . Equation (4) can then be replaced by the equation

$$(25) \quad \frac{dz}{dt} = A_0 \left( \frac{1 + FS}{1 + GS} \right) (B - z) - Sz.$$

Let us use (25) to compute the steady-state response  $T = Sz$  to a sustained signal  $S$ . We find that

$$(26) \quad T = \frac{PS(1 + QS)}{1 + RS + US^2}$$

where

$$P = B$$

$$(27) \quad Q = F = (A_0 + E)DA_0^{-1}C^{-1}$$

$$(28) \quad R = A_0^{-1} + F = A_0^{-1}[1 + (A_0 + E)DC^{-1}]$$

and

$$(29) \quad U = GA_0^{-1} = DA_0^{-1}C^{-1}.$$

Note that the form of (16) does not change if  $S$  is related to light intensity  $I$  by a law of the form

$$(30) \quad S(I) = \frac{\mu I}{1 + \nu I}.$$

Only the coefficients  $P$ ,  $Q$ ,  $R$ , and  $U$  change.

## 6. Turn-around of potential peaks at high background intensities

Despite the assumption that  $A$  depends on  $S$ , all of our explanations thus far use a *single* differential Equation (25). We will qualitatively explain the turn-around of potential peaks, the quenching of a second overshoot in double flash experiments, and the existence of rebound hyperpolarization when a depolarizing current is shut off during a hyperpolarizing light using only this differential

equation. In the BHL theory, by contrast, a substantial number of auxiliary differential equations are needed to explain all of these phenomena at once. Moreover, we can quantitatively fit the data using only Equation (25) better than BHL can fit the data using all their auxiliary variables. Our full theory provides an even better fit. More importantly, Equation (25) suggests that all these phenomena are properties of a transmitter gate.

To qualitatively explain the turn-around of peak potential as background intensity increases, we consider Figures 5 and 6.

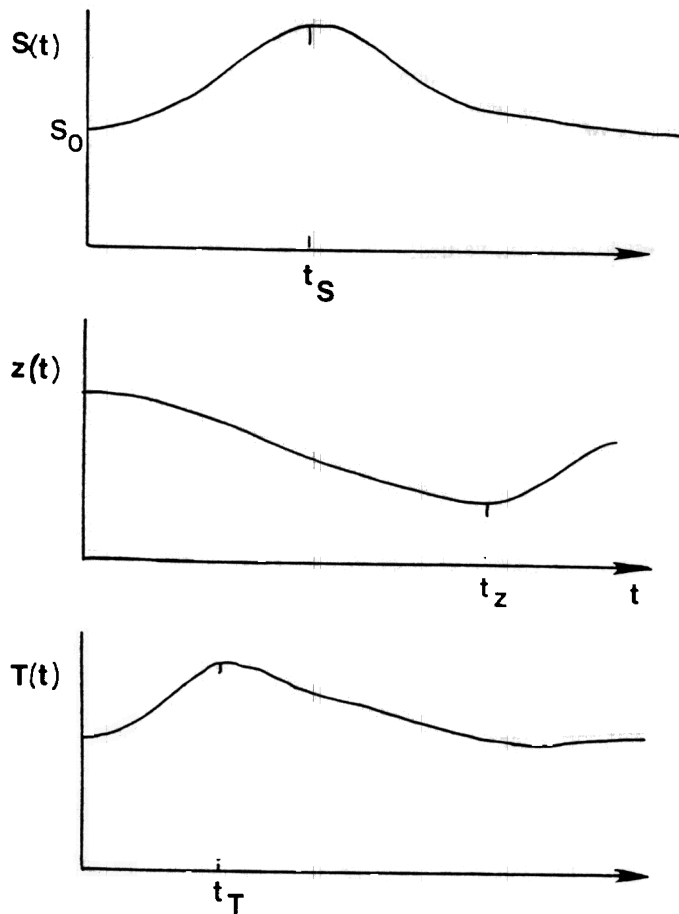


Fig. 5. Signal  $S(t)$  peaks at time  $t = t_s$  before transmitter  $z(t)$  reaches its minimum at time  $t = t_z$ . Consequently, the gated signal  $T = Sz$  peaks at a time  $t = t_T$  earlier than  $t = t_s$ .

In Figure 5,  $S$  starts out at a steady-state value  $S_0$ . Then a flash causes a chain reaction which creates a gradual rise and then fall in  $S$ . Function  $S$  reaches its maximum at the time  $t = t_s$  when  $dS/dt = 0$ . The transmitter  $z$  responds to the

increase in  $S$  by gradually being depleted. As the chain reaction wears off,  $z$  gradually accumulates again. Function  $z$  reaches its minimum at the time  $t = t_z$  when  $dz/dt = 0$ . From Figure 5, we can conclude that the gated signal  $T = Sz$  reaches a maximum at a time  $t = t_T$  before  $S$  reaches its maximum. This is because

$$(31) \quad \frac{dT}{dt} = \frac{dS}{dt}z + S\frac{dz}{dt}.$$

After time  $t = t_S$ , both  $dS/dt$  and  $dz/dt$  are negative until the chain reaction wears off. Thus  $dT/dt$  is also negative during these times. Consequently  $dT/dt = 0$  at a time  $t_T < t_S$ .

Figure 6 explains the turn-around by plotting the times when  $dS/dt = 0$ ,  $dz/dt = 0$ , and  $dT/dt = 0$  as a function of the background level  $S_0$ . In Figure 6, we think of  $t_S(S_0)$ ,  $t_z(S_0)$  and  $t_T(S_0)$  as functions of  $S_0$ . Two properties control the turn-around:

- (a) the function  $t_S(S_0)$  might or might not decrease as  $S_0$  increases, but eventually it must become approximately constant at large  $S_0$  values;
- (b) the function  $t_z(S_0)$  decreases faster as  $S_0$  increases until  $t_z(S_0)$  approximately equals  $t_S(S_0)$  at large  $S_0$  values.

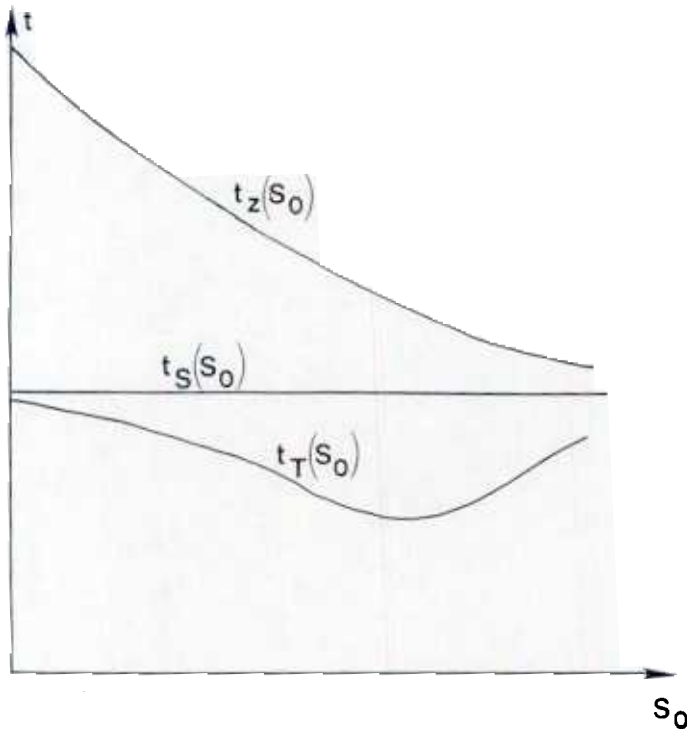


Fig. 6. As  $t_z(S_0)$  is drawn closer to  $t_S(S_0)$  at large  $S_0$  values due to enzymatic activation of transmitter accumulation rate,  $t_T(S_0)$  reaches a minimum and begins to increase again.

Property (a) is due to the fact that the photoreceptor has a finite capacity for reacting to photons in a unit time interval. After this capacity is exceeded, higher photon intensities cannot be registered. Property (b) is due to the light-induced increase of  $z$ 's reaction rate to higher  $S_0$  levels. Light speeds up  $z$ 's reaction rate, so that at higher  $S_0$  values  $z$  can equilibrate faster to the chain reaction  $S$ . In particular,  $t_z(S_0)$  approaches  $t_s(S_0)$  as  $S_0$  increases.

Using properties (a) and (b), we will now explain the turn-around. When  $S_0$  is small,  $dz/dt$  is also small. By (31) this means that  $dT/dt = 0$  almost when  $dS/dt = 0$ , or that  $t_T \cong t_s$ . As  $S_0$  increases to intermediate values, the chain reaction  $S$  also increases. Consequently  $dz/dt$  becomes more negative and makes  $z$  smaller. Also  $z$ 's gain is sped up, so that  $t_z$  approaches closer to  $t_s$ . In (31), this means that  $Sdz/dt$  will be large and negative at times when  $z$  is small. To achieve  $dT/dt = 0$ , we therefore need  $dS/dt$  to be large and positive. In other words,  $T$  reaches its peak while  $S$  is still growing rapidly. Hence  $t_T$  occurs considerably earlier than  $t_s$ . This argument shows why the peak of  $T$  occurs earlier as  $S_0$  increases.

Why does turn-around occur? Here properties (a) and (b) are fully used. By property (b),  $z$  reaches its minimum right after  $S$  reaches its maximum if  $S_0$  is large. In other words,  $t_z$  approaches  $t_s$  as  $S_0$  becomes large. This means that both  $dS/dt = 0$  and  $dz/dt = 0$  at almost the same time. By (31), also  $dT/dt = 0$  at about this time. In all,  $t_T \cong t_s \cong t_z$  if  $S \gg 0$ . Now we use property (a). Since  $t_s(S_0)$  is approximately constant at large  $S_0$  values,  $t_T(S_0)$  must bend backwards from its position much earlier than  $t_s(S_0)$  at intermediate  $S_0$  values to a position closer to  $t_s(S_0)$  values. This is the turn-around that we seek.

## 7. Double-flash experiments

In BHL's double flash experiments, a bright flash causes the potential to overshoot. A second bright flash that occurs while the potential is reacting to the chain reaction caused by the first flash does not cause an overshoot even though it extends the duration of the chain reaction. This effect can be explained as follows (Figure 7).

The first bright flash causes an overshoot due to the slow reaction of  $z$  to the onset of the chain reaction, as in Section 4. For definiteness suppose that  $z(0) = B$  at time  $t = 0$  and that the chain reaction starts rising at time  $t = 0$  to a maintained intensity of approximately  $S$ . By (16),  $z(t)$  decreases from  $B$  to approximately

$$(32) \quad \frac{B(1 + QS)}{1 + RS + US^2}.$$

This decrease in  $z(t)$  causes the overshoot, since the product  $Sz(t)$  first increases due to the fast increase in  $S(t)$  and then decreases due to the slower decrease in  $z(t)$ . Once  $z(t)$  equilibrates at the level (32), it thereafter maintains this level until the chain reaction decays. In a double-flash experiment, the second flash occurs before the chain reaction can decay. The second flash maintains the chain reaction

a while longer at the level  $S$ . No second overshoot in  $z$  occurs simply because  $z$  has already equilibrated at the level (32) by the time the second flash occurs.

When  $T$  is coupled to the potential  $V$ , the overshoot in  $T$  also causes a gain change in  $V$ 's reaction rate. BHL noticed this gain change and introduced another conductance into their model whose properties were tailored to explain the double flash experiment. In the BHL model, this second conductance is a rather mysterious quantity (see Section 15). In our model, it follows directly from the slow fluctuation rate of the transmitter gate (Section 9).

Our model's predictions can be differentiated from those of the BHL model because they all depend on the slow rate of the transmitter gate. Speeding up the transmitter's reaction rates should eliminate not only the overshoot and the second conductance, but also the photoreceptor's ability to remember an adaptational baseline (Section 3).

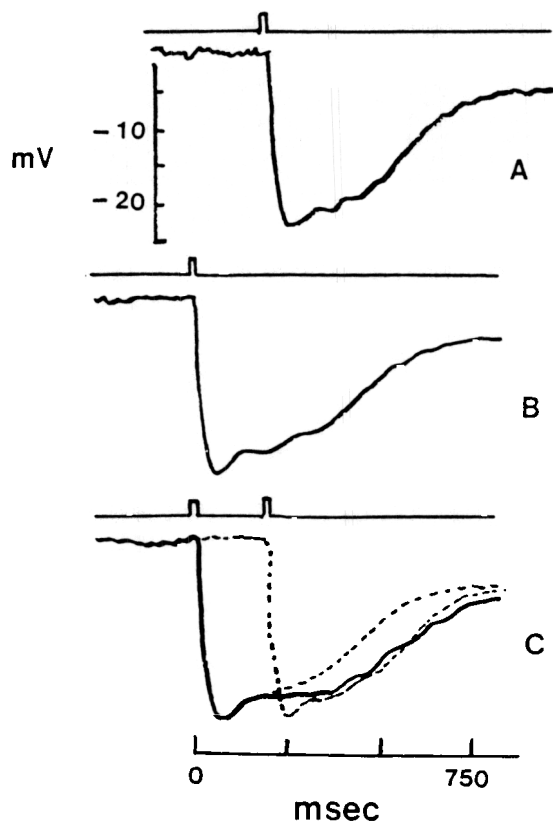


Fig. 7. Effect of a bright conditioning flash on the response to a subsequent bright test flash. (a) Response to test flash alone. (b) Response to conditioning flash alone. (c) Response to both flashes, with the upper two responses dotted. Redrawn from Fig. 15 of Baylor *et al.* (1974a), p. 716.

### 8. Antagonistic rebound by an intracellular dipole: rebound hyperpolarization due to current offset

The ubiquity of the gating design in neural systems is illustrated in a striking way by the following data. Baylor *et al.* (1974a) showed that offset of a rectangular pulse of depolarizing current during a cone's response to light causes a rebound hyperpolarization of the cone's potential. By contrast, offset of a depolarizing current in the absence of light does not cause a rebound hyperpolarization (Figure 8). In other words, an antagonistic rebound in potential, from depolarization to hyperpolarization, can sometimes occur.

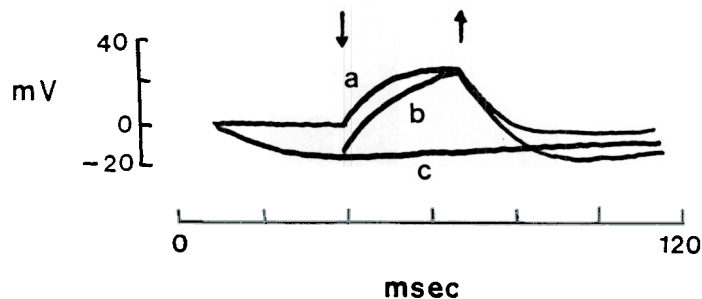


Fig. 8. Changes in potential produced by current in darkness (a), and during the response to light (b), superimposed tracings. Between arrows, a rectangular pulse of depolarizing current (strength  $1.5 \times 10^{-10}$ ) was passed through the microelectrode. (c) is the response to light without current. Redrawn from Fig. 10 of Baylor *et al.* (1974a), p. 706.

One of the most important properties of a slow gate is its antagonistic rebound property. This property was first derived to explain data about reinforcement and attention in Grossberg (1972a,b; 1975) and was later used to explain data about perception and cognitive development in Grossberg (1976, 1980). These results show how antagonistic rebounds can be caused when the signals to one or both of two parallel channels are gated before the gated signals compete to elicit net outputs from the channels (Figure 9). In reinforcement and cognitive examples, the two competing channels have typically been interpreted to be due to intercellular interactions. The competing channels implicated by the BHL data are, by contrast, intracellular. They are the depolarizing and hyperpolarizing voltage-conductance terms in the membrane equation for the cone potential (Section 9).

In the remainder of this section, we will review how slow gates can cause antagonistic rebounds. Then we will have reached the point where the gated signal must be coupled to the potential in order to derive further insights. This coupling is, however, quite standard in keeping with our claim that most of the interesting properties of the BHL data are controlled by the fluctuations of  $T$  under particular circumstances.

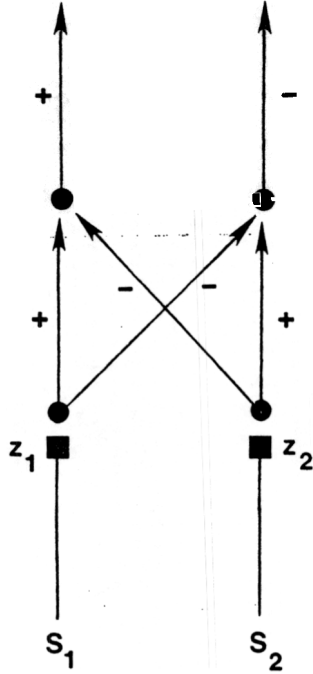


Fig. 9. A gated dipole. Signals  $S_1$  and  $S_2$  are gated by the slow transmitters  $z_1$  and  $z_2$  respectively, before the gated signals  $T_1 = S_1 z_1$  and  $T_2 = S_2 z_2$  compete to generate a net reaction.

To explain the main idea behind antagonistic rebound, suppose that one channel receives input  $S_1$  and that the other channel receives input  $S_2 = S_1 + \varepsilon$ ,  $\varepsilon > 0$ . Let the first channel possess a slow gate  $z_1$  and the second channel possess a slow gate  $z_2$ . Suppose for definiteness that each gate satisfies

$$(33) \quad z_i = \frac{P(1 + QS_i)}{1 + RS_i + US_i^2},$$

$i = 1, 2$ , as in (32). The explicit form of (33) is irrelevant. All we need is the property that  $z_i$  is a decreasing function of  $S_i$ . In other words, larger signals can deplete more transmitter. This is true in (33) because, by (27) and (28),  $Q < R$ .

However, the opposite is true for the gated signals  $T_1 = S_1 z_1$  and  $T_2 = S_2 z_2$ . The function

$$(10) \quad T = \frac{PS(1 + QS)}{1 + RS + US^2}$$

is an *increasing* function of  $S$  because, by (27)–(29)  $QR > U$ . In other words, a larger  $S$  signal produces a larger output  $T$  even though it depletes more  $z$ . This simple yet subtle fact about gates lies at the heart of our explanation of antago-

nistic rebound. The property was first derived in Grossberg (1968, 1969). The lack of widespread knowledge of this property among experimentalists has caused much unnecessary confusion about the dynamics of transmitters in various neural systems. Because this fact was not known to BHL, they found an ingenious, albeit unintuitive, way to explain the rebound in terms of their second conductance. Our theory differs from theirs strongly on this point. Their steady-state Equation (18) does not embody either the intuitive meaning or the mathematical properties of our steady-state Equation (16).

In our theory, antagonistic rebound can be trivially proved as follows. When  $\varepsilon$  is on,  $S_2 > S_1$ . Consequently, despite the fact that  $z_2 < z_1$ , it follows that  $T_2 > T_1$ . After competition acts, the net output  $T_2 - T_1$  of the on-channel is positive. To see how rebound occurs, shut  $\varepsilon$  off. Then  $S_2$  and  $S_1$  rapidly equalize at the value  $S_1$ . However  $z_2$  and  $z_1$  change more slowly. Thus the inequality  $z_2 < z_1$  persists for some time. Consequently the net output reverses sign because

$$(34) \quad T_2 - T_1 \cong S_1(z_2 - z_1) < 0$$

and an antagonistic rebound occurs. The rebound is transient due to the fact that  $z_2$  and  $z_1$  gradually equilibrate to the same input  $S_1$  at a common value  $z_1$ , and thus

$$(35) \quad T_2 - T_1 \cong S_1 z_1 - S_1 z_1 = 0$$

after equilibration occurs. A similar argument shows how antagonistic rebound can occur if only the channel whose input is perturbed contains a slow gate.

### 9. Coupling of gated input to the photoreceptor potential

The photoreceptor potential  $V$  is assumed to obey the standard membrane equation

$$(36) \quad C_0 \frac{dV}{dt} = (V^+ - V)g^+ + (V^- - V)g^- + (V^p - V)g^p$$

where  $V(t)$  is a variable voltage;  $C_0$  is a capacitance;  $V^+$ ,  $V^-$ , and  $V^p$  are excitatory, inhibitory, and passive saturation points, respectively;  $g^+$ ,  $g^-$ , and  $g^p$  are excitatory, inhibitory, and passive conductances, respectively; and

$$(37) \quad V^- \leq V^p < V^+.$$

Then  $V^- \leq V(t) \leq V^+$  for all  $t \geq 0$  if  $V^- \leq V(0) \leq V^+$ . By rewriting (36) as

$$(38) \quad C_0 \frac{dV}{dt} = -(g^+ + g^- + g^p)V + V^+g^+ + V^-g^- + V^p g^p$$

we notice that the total gain of  $V$  is  $g^+ + g^- + g^p$  and the asymptote of  $V$  in response to constant conductances is

$$(39) \quad \frac{V^+g^+ + V^-g^- + V^p g^p}{g^+ + g^- + g^p}$$

Both the gain and the asymptote are altered by changing the conductances. In the special case of the turtle cone, light acts by decreasing the excitatory conductance  $g^+$  (Baylor *et al.*, 1974b). We will assume below that the gated signal  $T$  causes this change in  $g^+$ . Light hereby slows down the cone's reaction rate as it hyperpolarizes the cone (driving  $V$  towards  $V^-$ ). We wish to emphasize at the outset that similar results would hold if we assumed that  $T$  increased, rather than decreased,  $g^+$ . The main difference would be a speeding up of the potential change rather than its slowing down by inputs  $T$ . In all situations wherein  $V$  can react more quickly than  $T$  can fluctuate, differences in the gain of  $V$  do not imply new qualitative properties, although they can imply quantitative differences. One of these differences is that a decrease of  $V$ 's gain as  $T$  increases prolongs the duration of  $V$ 's reaction to light.

We will couple  $T$  to  $g^+$  using a simple mass action law. Suppose that there exist  $g_0$  membrane 'pores' of which  $g^+ = g(t)$  pores are open and  $g_0 - g(t)$  are closed at any time  $t$ . Suppose that  $T$  closes open pores by mass action, so that  $g_0$  pores will open after  $T$  shuts off. Then

$$\frac{dg}{dt} = H(g_0 - g) - JgT$$

where  $H$  and  $J$  are positive constants. Suppose also that this process is rapid compared to  $V$ 's reaction rate to changes in  $g$ . We can then assume that  $g$  is always in approximate equilibrium with  $T$ . Setting  $dg/dt = 0$ , we find

$$(41) \quad g^+ = \frac{g_0}{1 + KT}$$

where  $K = JH^{-1}$ . To achieve a more symmetric notation, we write  $g^- = g_1$  and for simplicity set  $g^p = 0$ . We also rescale the time variable so that  $C_0 = 1$  in (36). Then Equation (36) takes the form

$$(42) \quad \frac{dV}{dt} = (V^+ - V) \frac{g_0}{1 + KT} - (V - V^-)g_1.$$

Our next steps are to compute the equilibrium potential  $V_0$  that occurs when  $T = 0$ , and to write an equation for the amount of hyperpolarization

$$(43) \quad x = V_0 - V$$

that occurs in response to an arbitrary function  $T$ . We find

$$(44) \quad V_0 = \frac{V^+g_0 + V^-g_1}{g_0 + g_1}$$

and

$$(45) \quad \frac{dx}{dt} = - \left[ g_1 + \frac{g_0}{1 + KT} \right] x + \frac{LT}{1 + KT}$$

where

$$L = Kg_1(V_0 - V^-).$$

The steady-state value  $x_\infty$ , of  $x$ , in response to a constant or slowly varying  $T$  is found by (45) to be

$$x_\infty = \frac{MT}{N + T}$$

where

$$M = V_0 - V^- > 0$$

and

$$N = (g_0 + g_1)g_1^{-1}K^{-1}$$

From (47), it follows that

$$\frac{Nx_\infty}{M - x_\infty} = T$$

where  $M$  is the maximum possible level of hyperpolarization. This equation is formally identical to the BHL equation (in their notation)

$$(51) \quad \frac{aU}{U_L - U} = \frac{z_1}{K}$$

except that their blocking variable  $z_1$  is replaced by our gated signal  $T = Sz$  (Baylor *et al.*, 1974b). The formal similarity of (50) to (51) is one cornerstone on which our fit to the BHL data is based. Another cornerstone is the fact that  $T$  satisfies the equation

$$(16) \quad T = \frac{PS(1 + QS)}{1 + RS + US^2}$$

whereas  $z_1$  satisfies

$$\frac{z_1}{K} = \frac{PS(1 + QS)}{1 + RS}$$

BHL relate data about  $U$  to data about  $S$  via the hypothetical process  $z_1$  using (18) and (51) just as we relate data about  $x$  to data about  $S$  via the hypothetical process  $T$  using (16) and (50). Despite these formal similarities, the substantial differences between other aspects of the two theories show how basic the gating concept is in transmitter dynamics.

### 10. 'Extra' slow conductance during overshoot and double flash experiments

Baylor *et al.* (1974a) found that a bright flash causes an overshoot in hyperpolarization followed by a plateau phase before the potential returned to its baseline level. They also found that an extra conductance accompanies the overshoot. Because their blocking and unblocking variables could not explain these overshoot and conductance properties, they added a new conductance term, denoted  $G_f$ , to their voltage equation and defined its properties to fit the data. Baylor *et al.* (1974b) also defined the properties of  $G_f$  to explain double flash experiments. If a second bright flash occurs during the plateau phase of the response to the first flash, then the plateau phase is prolonged, but a second overshoot does not occur (Figure 7).

We will argue that such an 'extra' conductance follows directly from the coupling of the gated signal  $T$  to the potential  $V$ . In other words, an extra conductance can be measured without postulating the existence of an extra membrane channel to subserve this conductance.

To qualitatively understand this property, note that the gain of  $x$  in (45) is

$$(49) \quad \Gamma = \frac{g_0 + g_1 + g_1 KT}{1 + KT}.$$

Approximate the chain reaction that is elicited by a bright flash with a rectangular step

$$S(t) = \begin{cases} 0 & \text{if } t < 0, \\ S & \text{if } t \geq 0. \end{cases}$$

Then (25) and (53) imply  $z(t) = B$  for  $t < 0$ , whereas

$$(50) \quad z(t) = Be^{-[A(S)+S]t} + \frac{BA(S)}{A(S) + S} (1 - e^{-[A(S)+S]t})$$

for  $t \geq 0$ , where

$$(55) \quad A(S) = A_0 \left[ \frac{1 + FS}{1 + GS} \right].$$

Equation (54) can be rewritten as

$$(56) \quad z(t) = \frac{BA(S)}{A(S) + S} + \frac{BS}{A(S) + S} e^{-[A(S)+S]t}.$$

Thus  $z$  reacts to the chain reaction with a fast component  $BA(S)[A(S) + S]^{-1}$  and a slowly decaying component  $BS[A(S) + S]^{-1} \exp[-(A(S) + S)t]$ . The slow component causes an overshoot in  $T = Sz$ , and thus in  $x$ 's asymptote  $MT(N + T)^{-1}$ . The gain  $\Gamma$  of  $x$  also possesses fast and slow components. We identify the slow component of  $\Gamma$  with the extra conductance that BHL observed. Note that the same process which causes the overshoot of  $x$  also causes the

emergence of the slow conductance; namely, the slow equilibration of  $z(t)$  to the new level of the chain reaction.

This explanation easily shows not only why a second flash (Figure 7) does not create another overshoot, but also why the slow component in the gain of  $x$  does not reappear in response to a second flash. In the BHL model, this slow conductance and its relationship to the overshoot had to be added to the theory to fit the data. In the gating model, the slow component and its relationship to the overshoot occur automatically.

An estimate of  $\Gamma$  as a sum of constant, fast, and slow conductances can be computed by using the approximation

$$(57) \quad \frac{1}{1 + KT} \cong 1 - KT + K^2T^2 - K^3T^3$$

to rewrite (52) as

$$(58) \quad \Gamma \cong g_0 + g_1 - g_0KT + g_0K^2T^2 - g_0K^3T^3.$$

Then substitute

$$T = \frac{BSA(S)}{A(S) + S} + \frac{BS^2}{A(S) + S} e^{-[A(S)+S]t}$$

into (58), and segregate constant, fast, and slow terms. This computation is unnecessary, however, to understand the qualitative reasons for correlated overshoot and gain changes.

## 11. Shift property and its relationship to enzymatic modulation

An important property of certain isolated photoreceptors is their ability to shift their operating range of maximal sensitivity, without compressing their full dynamic range, in response to shifts in background light intensity (Figure 10). Such a shift property can be caused by the action of shunting lateral inhibition within a network of cells (Grossberg 1978*a,b*). Herein we show how it can be caused when a transmitter gate reacts to changes in light level more slowly than the light-mediated chain reaction that causes transmitter release. The result also predicts a relationship between the amount of shift and the influence of light on the enzymatic activation of transmitter at high light intensities. By Section 5, the amount of shift should also be related to the size of the turn-around in the timing of potential peaks to fixed flashes on increasing background intensities.

The result follows from (47). Suppose that  $z_0$  has equilibrated to a steady background level  $S_0$  so that

$$(60) \quad z_0 = \frac{P(1 + QS_0)}{1 + RS_0 + US_0^2}$$

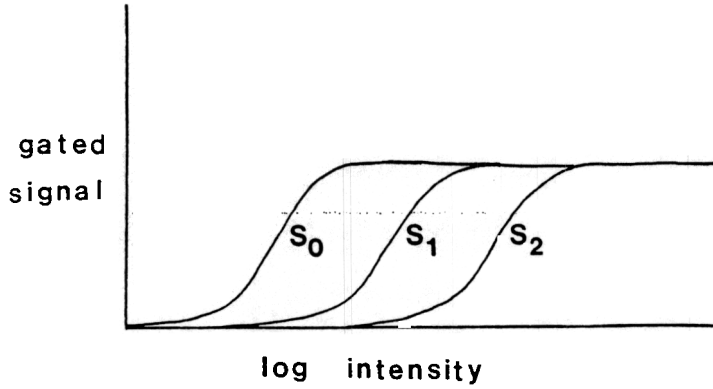


Fig. 10. Shift of dynamic range to increments in  $\log S$  after transmitter equilibrates to different background intensities  $S_0, S_1, S_2, \dots$

as in (33). Now parametrically change the input level  $S$  and measure the hyperpolarization  $x$  a fixed time after the change in  $S$  and before  $z$  can substantially change. For simplicity, denote the series of  $S$  values at this time by  $S^{(0)}$  and the corresponding hyperpolarizations by

$$(61) \quad x^{(0)} = \frac{MS^{(0)}z_0}{N + S^{(0)}z_0}.$$

Also perform the same experiment using a different background level  $S_1$  that causes a different  $z$  level

$$z_1 = \frac{P(1 + QS_1)}{1 + RS_1 + US_1^2}$$

and a different series of hyperpolarizations

$$(62) \quad x^{(1)} = \frac{MS^{(1)}z_1}{N + S^{(1)}z_1}$$

in response to the test inputs  $S^{(1)}$ . The theoretical question to be answered is the following. If the series of test inputs  $S^{(0)}$  and  $S^{(1)}$  are plotted in logarithmic coordinates does the series  $x^{(0)}$  differ from the series  $x^{(1)}$  by a constant shift  $\lambda$ ? In other words, if we write  $S^{(0)} = e^K$  and  $S^{(1)} = e^{K+\lambda}$ , is

$$(64) \quad x^{(1)}(K + \lambda) \equiv x^{(0)}(K)$$

for all  $K \geq 0$  and a suitable choice of  $\lambda$ ? A simple computation answers this question in the affirmative with

$$\lambda = \ln \left( \frac{z_0}{z_1} \right).$$

The effect of light-induced enzymatic activation of  $z$  on  $\lambda$  is controlled by the quadratic terms  $US_0^2$  and  $US_1^2$  in (60) and (62), respectively. Without enzymatic activation,  $U=0$ . Thus as  $S_0 \rightarrow \infty$  and  $S_1 \rightarrow \infty$ , both  $z_0$  and  $z_1$  approach  $PQR^{-1}$ , so  $\lambda \rightarrow 0$ . By contrast, if  $U > 0$ , then at large values of  $S_0$  and  $S_1$ ,

$$(66) \quad \lambda \sim \ln \left( \frac{S_1}{S_0} \right).$$

Consequently by choosing a series of background inputs  $S_0$  and  $S_1$  such that  $S_1 = MS_0$ , an asymptotic shift  $\lambda$  of size  $\ln(M)$  can be achieved. Of course, all of these estimates are approximate, since  $z$  begins to adapt to the new level of  $S$  as soon as  $S$  changes the chain reaction,  $z$ 's adaptation rate depends on  $S$ , and  $S$  can asymptote at a finite level whether or not  $U = 0$  because the photoreceptor possesses only finitely many receptors with which to bind photons. Nonetheless, the qualitative relationship between asymptotic  $\lambda$  values and the highest power of  $S$  in the steady-state equation for  $z$  is worth noting as a possible tool for independently testing whether an experimental manipulation has altered the enzymatic step.

## 12. Rebound hyperpolarization, antagonistic rebound, and input doubling

The rebound hyperpolarization depicted in Figure 9 can be explained using Equation (42); namely,

$$(42) \quad \frac{dV}{dt} = (V^+ - V) \frac{g_0}{1 + KT} - (V - V^-)g_1.$$

Rebound hyperpolarization can be explained if the depolarizing pulse interferes with the ability of the signal  $S$  in the  $g^+$  channel to release transmitter. This suggestion is compatible with the data in Figure 9, since the depolarizing pulse acting by itself achieves the same depolarization as the pulse acting together with hyperpolarizing light. We therefore suppose that the effective signal strength during a depolarizing pulse of intensity  $J$  is  $\theta S$ , where the function  $\theta = \theta(J)$  is a non-negative decreasing function of  $J$  such that  $\theta(0) = 1$  and  $\theta(J) \ll 1$  if  $J \gg 0$ . To see how this mechanism works, suppose that  $S(t)$  is a rectangular step with onset time  $t = 0$  and intensity  $S$ . After the light and the depolarizing pulse are both turned on,  $z(t)$  will approach the asymptote

$$(67) \quad \frac{P(1 + Q\theta S)}{1 + R\theta S + U\theta^2 S^2}$$

rather than the smaller asymptote

$$(68) \quad \frac{P(1 + QS)}{1 + RS + US^2}$$

that would have been approached in the absence of the depolarizing current. If  $\theta$

is small, the asymptote of  $V$  with and without current will be similar because the gated signal

$$(69) \quad T = \frac{\theta SP(1 + Q\theta S)}{1 + R\theta S + U\theta^2 S^2}$$

approaches zero as  $\theta$  does. If the pulse is shut off at time  $t = t_0$ ,  $\theta$  rapidly returns to the value 1, so that  $S$  can bind transmitter with its usual strength. Hence shortly after time  $t = t_0$ , the gated signal will approximately equal

$$(70) \quad T_\theta = \frac{SP(1 + QS)}{1 + RS + US^2}$$

by (68), rather than the smaller value

$$(71) \quad T_1 = \frac{SP(1 + QS)}{1 + RS + US^2}$$

that it would have attained by (68), had the depolarizing pulse never occurred. By (70), (71), and (42), more hyperpolarization occurs after the current is shut off than would have occurred in response to the light alone.

This explanation of rebound hyperpolarization can be tested by doing parametric studies in which the asymptote of  $V$  in response to a series of  $J$  values is used to estimate  $\theta(J)$  from (42) and (69). When this  $\theta(J)$  function is substituted in (70), a predicted rebound hyperpolarization can be estimated by letting  $T = T_\theta$  in (42).

A related rebound hyperpolarization effect can be achieved if, after the photo-receptor equilibrates to a fixed background level  $S$ , a step of additional input intensity is imposed for a while, after which the input is returned to the level  $S$ . An overshoot in potential to step onset, and an undershoot in potential to step offset, as well as a slowing down of the potential gain, can all be explained using (42) augmented by a transmitter gating law. Kleinschmidt and Dowling (1975) have measured such an effect in the *Gekko gekko* rod. It can be explained using Figure 11. Figure 11a depicts the (idealized) temporal changes in the input signal  $S(t)$ ; Figure 11b depicts the corresponding depletion and recovery of  $z(t)$ , and Figure 11c depicts the consequent overshoot and undershoot of the gated signal  $T(t)$ , which has corresponding effects on the asymptote and gain of the potential  $V(t)$ .

Baylor *et al.* (1974a, p. 714) did a related experiment when they either interrupted or brightened a steady background light. In particular, they first exposed the turtle eye to a light equivalent to  $3.7 \times 10^4$  photon  $\mu\text{m}^{-2} \text{sec}^{-1}$  for one second. Then the light intensity was either doubled or reduced to zero for 40 msec. The net effect is to add or subtract the same light intensity from a steady background. The depolarization resulting from the offset of light is larger than the hyperpolarization resulting from doubling the light. This follows from (42) by showing that the equilibrium hyperpolarization achieved by setting  $S = S_0$

is greater than the change in hyperpolarization achieved right after switching  $S$  to  $2S_0$  given that the transmitter has equilibrated to  $S = S_0$ . In other words,

$$(72) \quad \frac{a}{c} - \frac{a + \alpha b}{c + b} > \frac{a + \alpha b}{c + b} - \frac{a + 2\alpha b}{c + 2b}$$

where

$$(73) \quad a = g_0 V^+ + g_1 V^-$$

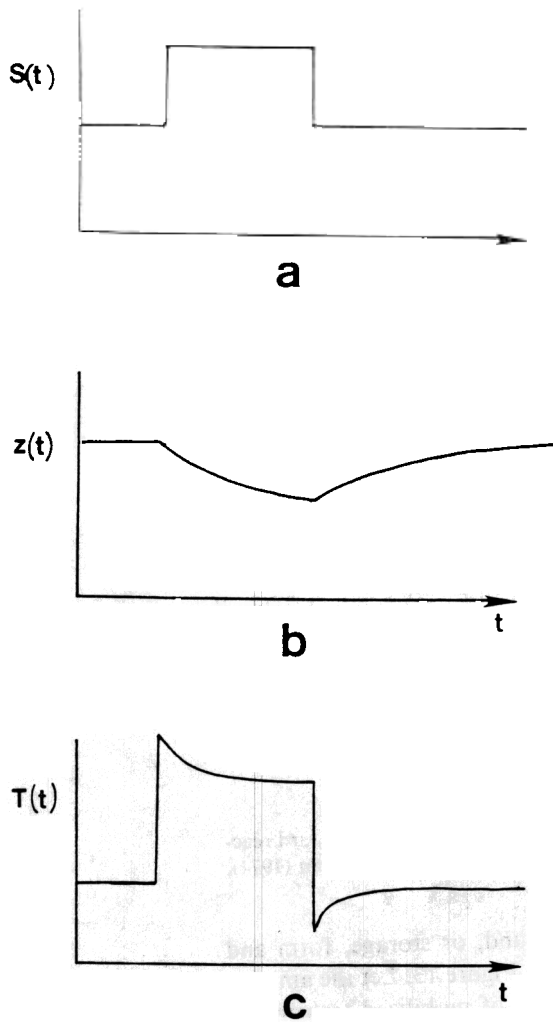


Fig. 11. (a) Rectangular step in  $S(t)$  causes (b) gradual depletion-then-accumulation of  $z(t)$ . The combined effect is (c) overshoot and undershoot of  $T(t)$ .

$$(74) \quad b = g_1 K S_0 z_0$$

$$(75) \quad c = g_0 + g_1$$

and

$$(76) \quad \alpha = V^-$$

Inequality (72) can be reduced to the inequality  $V^+ > V^-$ , and is therefore true. Another inequality follows from  $V^+ > V^-$  and is stated as a prediction. Twice the equilibrium hyperpolarization achieved by setting  $S = S_0$  exceeds the total hyperpolarization achieved right after switching  $S$  to  $2S_0$  given that the transmitter has equilibrated to  $S = S_0$ . In other words,

$$(77) \quad 2\left(\frac{a}{c} - \frac{a + ab}{c + b}\right) > \frac{a}{c} - \frac{a + 2ab}{c + 2b}.$$

### 13. Transmitter mobilization

Baylor *et al.* (1974a) found that very strong flashes or steps of light introduce extra components into the response curves of the cone potential. These components led BHL to postulate the existence of more slow processes  $z_3$ ,  $z_4$ , and  $z_5$ , in addition to their blocking and unblocking variables  $z_1$  and  $z_2$ . The time scales which BHL ascribed to this augmented chain reaction of slow processes are depicted in Figure 12.

Below we will indicate how transduction processes that are familiar in other transmitter systems, say in the mobilization of acetylcholine at neuromuscular junctions (Eccles, 1964, p. 90f) or of calcium in the sarcoplasm reticulum of skeletal muscles (Caldwell, 1971), can account for the existence of extra components. We will also indicate how these processes can cause very small correction terms to occur in the steady-state relationship (16) between the gated signal  $T$  and the signal intensity  $S$ .

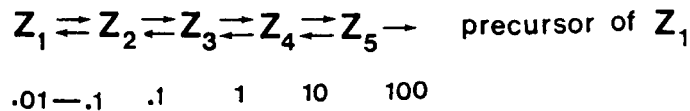


Fig. 12. Order of magnitude of the time constants of the  $z_i$  processes in seconds. Backward reactions are all small compared to forward reactions. Redrawn from Baylor and Hodgkin (1974), p. 757.

Let us distinguish between transmitter that is in bound, or storage, form and transmitter that is in available, or mobilized, form, as in Figure 13. Let the amount of storage transmitter at time  $t$  be  $w(t)$  and the amount of mobilized transmitter at time  $t$  be  $z(t)$ . We must subdivide the processes defining (4) among the components  $w(t)$  and  $z(t)$ , and allow storage transmitter to be mobilized and conversely. Then (4) is replaced by the system

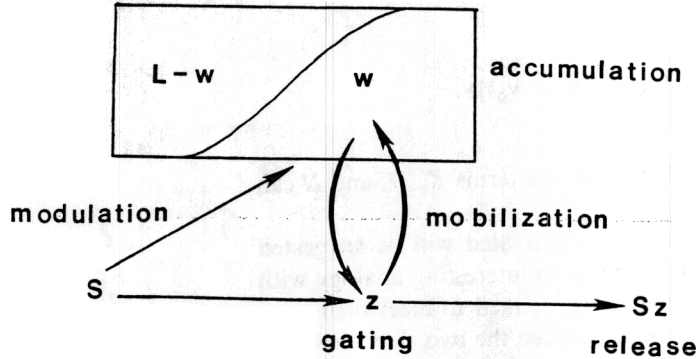


Fig. 13. Transmitter  $w$  accumulates until a target level is reached. Accumulated transmitter is mobilized until an equilibrium between mobilized and unmobilized transmitter fractions is attained. The signal  $S$  is gated by mobilized transmitter which is released by mass action. The signal also modulates the accumulation and/or mobilization processes.

$$(78) \quad \frac{dw}{dt} = K(L - w) - (Mw - Nz)$$

and

$$\frac{dz}{dt} = (Mw - Nz) - Sz.$$

Term  $K(L - w)$  in (78) says that  $w(t)$  tries to maintain a level  $L$  via transmitter accumulation (or production and feedback inhibition). Term  $-(Mw - Nz)$  in (78) says that storage transmitter  $w$  is mobilized at a rate  $M$  whereas mobilized transmitter  $z$  is demobilized and restored at a rate  $N$  until the two processes equilibrate. Term  $Mw - Nz$  in (79) says that  $w$ 's loss is  $z$ 's gain. Term  $-Sz$  in (79) says that mobilized transmitter is released at rate  $-Sz$  as it couples to the signal  $S$  by mass action. In all, Equations (78) and (79) are the minimal system wherein transmitter accumulation, gating, and release can occur given that transmitter must be mobilized before it can be released.

Once this system is defined, we must again face the habituation dilemma that was discussed in Section 5. Should not some or all of the production and mobilization terms be enzymatically activated by light to prevent the mobilized transmitter from being rapidly depleted by high intensity lights? The terms which are candidates for enzymatic activation in (78) and (79) are  $K$ ,  $M$ , and  $N$ , as in the equations

$$(80) \quad \frac{dK}{dt} = -\alpha_K(K - K_0) + \beta_K[\gamma_K - (K - K_0)]S,$$

$$(81) \quad \frac{dM}{dt} = -\alpha_M(M - M_0) + \beta_M[\gamma_M - (M - M_0)]S,$$

and

$$(82) \quad \frac{dN}{dt} = -\alpha_N(N - N_0) + \beta_N[\gamma_N - (N - N_0)]S.$$

The BHL data are insufficient to conclude whether all the terms  $K$ ,  $M$ , and  $N$  can vary due to light activation.

A possible empirical test of how many terms are activated will be suggested below. Before this test is described, however, we note an interesting analogy with the five slow variables  $z_1, z_2, z_3, z_4$ , and  $z_5$  that BHL defined to meet their data and the five slow variables  $w, z, K, M$ , and  $N$ . BHL needed the two slow variables  $z_1$  and  $z_2$  to fit their data at moderate light intensities, and the three extra variables  $z_3, z_4$ , and  $z_5$  to describe components at very high light intensities. By comparison, the variables  $w, z, K, M$ , and  $N$  are five slow variables with  $w$  and  $z$  the dominant variables at intermediate light intensities, and  $K, M$ , and  $N$  possibly being slowly activated at high light intensities. Apart from the similarity in the numbers of slow variables in the two models, their dynamics and intuitive justification differ markedly, since our variables have an interpretation in general transmitter systems, whereas the BHL variables were formally defined to fit their data.

A possible test of the number of enzymatically activated coefficients is the following. Recall that enzymatic activation of transmitter production changed the steady-state law relating  $T$  to  $S$  from (17) to (16). In other words, enzymatically activating one coefficient adds one power of  $S$  to both the numerator and the denominator of the law for  $T$ . Analogously, enzymatically activating  $n$  coefficients adds  $n$  powers of  $S$  to the numerator and denominator of this law. When  $n = 3$ , the law takes the form

$$(83) \quad T = \frac{P^*S(1 + Q^*S + R^*S^2 + U^*S^3)}{1 + V^*S + W^*S^2 + X^*S^3 + Y^*S^4}.$$

The higher-order coefficients  $R^*$ ,  $U^*$ ,  $X^*$ , and  $Y^*$  are very small compared to the other coefficients  $P^*$ ,  $Q^*$ ,  $V^*$ , and  $W^*$ . Thus the enzymatic activation terms add very small corrections to the high intensity values of  $T$ , and thus to the corresponding values of  $x_\infty$  via (50). If these high-intensity corrections could be measured, we would have an experimental test of how many terms  $K$ ,  $M$ , and  $N$  are enzymatically activated. These higher powers do not alter the asymptotic shift  $\lambda$  in (66), but they do alter the rate with which the asymptotic shift is approached as a function of increasing light intensity.

We have hereby qualitatively explained all the main features of the BHL data using a minimal model of a miniaturized chemical transmitter. It remains to comment more completely on the form of the chain reaction which we used to convert light intensity  $I(t)$  into the signal  $S(t)$  and to display quantitative data fits. The simplest chain reaction is the one used by BHL:

$$\left\{ \begin{array}{l} \frac{dy_1}{dt} + \gamma_1 y_1 = cI(t) \\ \frac{dy_2}{dt} + \gamma_2 y_2 = \gamma_1 y_1 \\ \\ \frac{dy_n}{dt} + \gamma_n y_n = \gamma_{n-1} y_{n-1} \end{array} \right.$$

$$S(t) = y_n(t).$$

We have used this chain reaction with good results. However, this law possesses the physically implausible property that  $y_i \rightarrow \infty$  as  $I \rightarrow \infty$ . Only finite responses are possible *in vivo*. A related chain reaction avoids this difficulty and also fits the data well. This modified chain reaction approximates (84) at small  $I(t)$  values. It is

$$(85) \quad \left\{ \begin{array}{l} \frac{dy_1}{dt} + \gamma y_1 = (\delta - \epsilon y_1)I(t) \\ \frac{dy_2}{dt} + \gamma y_2 = (\delta - \epsilon y_2)\gamma_1 y_1 \\ \\ \frac{dy_n}{dt} + \gamma y_n = (\delta - \epsilon y_n)\gamma_{n-1} y_{n-1} \end{array} \right.$$

$$S(t) = y_n(t).$$

It is easily checked that in response to a step of light of intensity  $I$ , all the asymptotes  $y_i(\infty)$  in (85) have the form  $\mu I(1 + \nu I)^{-1}$ , as in (30). The possibility exists that each step in this chain reaction is gated by a slow transducer. This would help to explain why so many slow variables appear at high light intensities even if not all the rates  $K$ ,  $M$ , and  $N$  are enzymatically activated. Such a complication of the model adds no new conceptual insights and will remain unwarranted until more precise biochemical data are available.

#### 14. Quantitative analysis of models

In this section we will compare the experimental measurements of Baylor and Hodgkin (1974) with the predictions of their model (Baylor *et al.*, 1974b) and our models I (Equation (25)) and II (Equations (4) and (19)). The BHL model is outlined in Section 15. For each of Models I:

$$(25) \quad \frac{dz}{dt} = A_0 \left[ \frac{1 + FS}{1 + GS} \right] (B - z) - Sz$$

and II:

$$(4) \quad \frac{dz}{dt} = A(B - z) - Sz$$

$$\frac{dA}{dt} = -C(A - A_0) + D[E - (A - A_0)]S,$$

we will examine the properties of the gated signal

$$(2) \quad T = Sz.$$

That is, we present a model in which the amount of hyperpolarization,  $x$ , is directly proportional to  $Sz - S_0z_0$ , where  $T_0 = S_0z_0$  is the steady-state level. Similar results, with better quantitative fits, are obtained when the potential obeys the equation

$$C_0 \frac{dV}{dt} = (V^+ - V) \frac{g_0}{1 + KT} - (V - V^-)g_1.$$

Recall that, if the potential obeys Equation (42), then the amount of hyperpolarization is given by the equation

$$(45) \quad C_0 \frac{dx}{dt} = - \left[ g_1 + \frac{g_0}{1 + KT} \right] x + \frac{LT}{1 + KT}$$

and, if  $x$  equilibrates quickly relative to  $z$ ,

$$(47) \quad x \cong \frac{MT}{N + T}.$$

Equation (47) says that  $x$  is approximately proportional to  $T$  if  $N$  is large relative to  $T$ .

For the rest of the section we will consider the experiment (Section 4) in which a short flash of fixed intensity is superimposed on ever-increasing levels of background light. Let  $x$  be the amount of hyperpolarization and  $x_0$  the equilibrium level for a fixed background intensity. As presented in Figure 3, the peak  $x - x_0$  decreases as background intensity increases, but the time at which the peak occurs first decreases and then increases as the intensity increases.

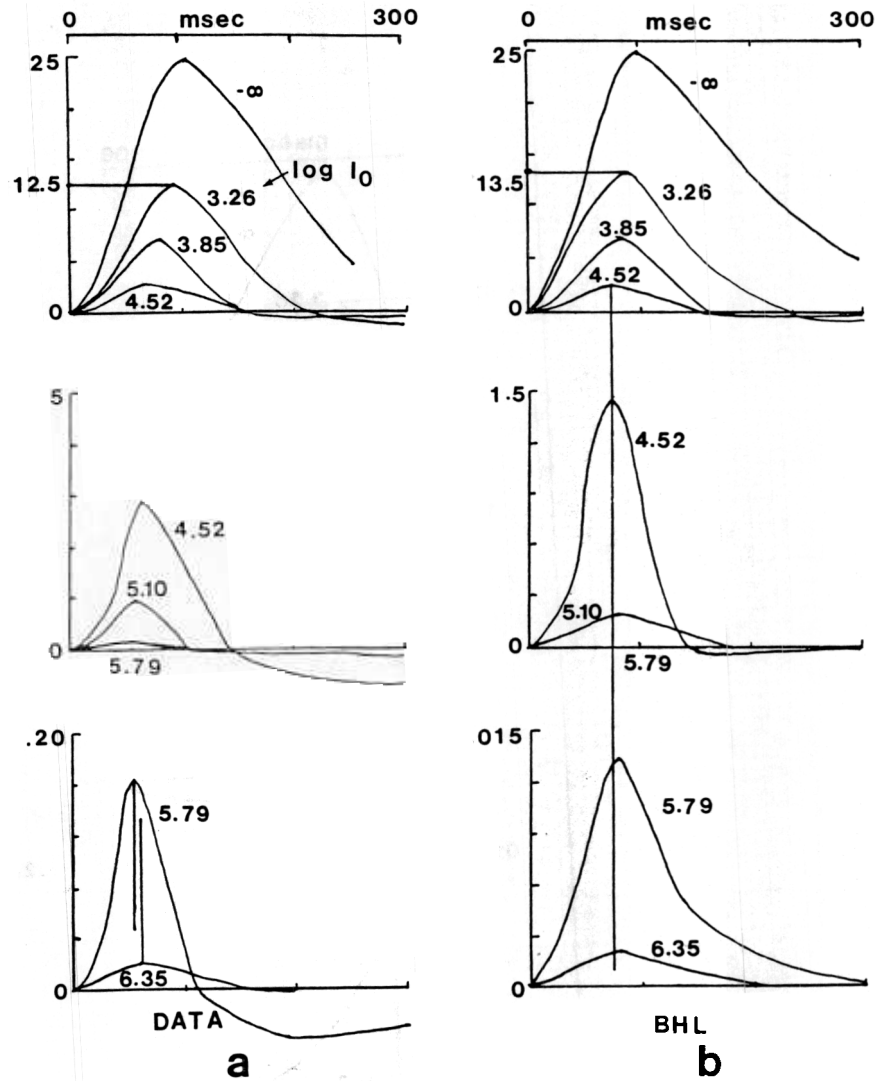


Fig. 14. Intracellular response curves  $x(t) - x_0$  showing the effect of a flash superimposed on a background light of fixed intensity. Each horizontal axis represents the time since the middle of the flash, which lasts 11 msec. The vertical axis is scaled so that the peak value of  $x(t) - x_0 = x(t)$  in the dark is equal to 25. The number above each curve is  $\log_{10} I_0$  of the background light intensity  $I_0$ , which is calibrated so that when  $\log_{10} I_0 = 3.26$ , the peak of  $x(t) - x_0$  is equal to 12.5. (a) The Baylor-Hodgkin (1974) data. (b) The BHL model (redrawn from Baylor *et al.* (1974b), p. 785).

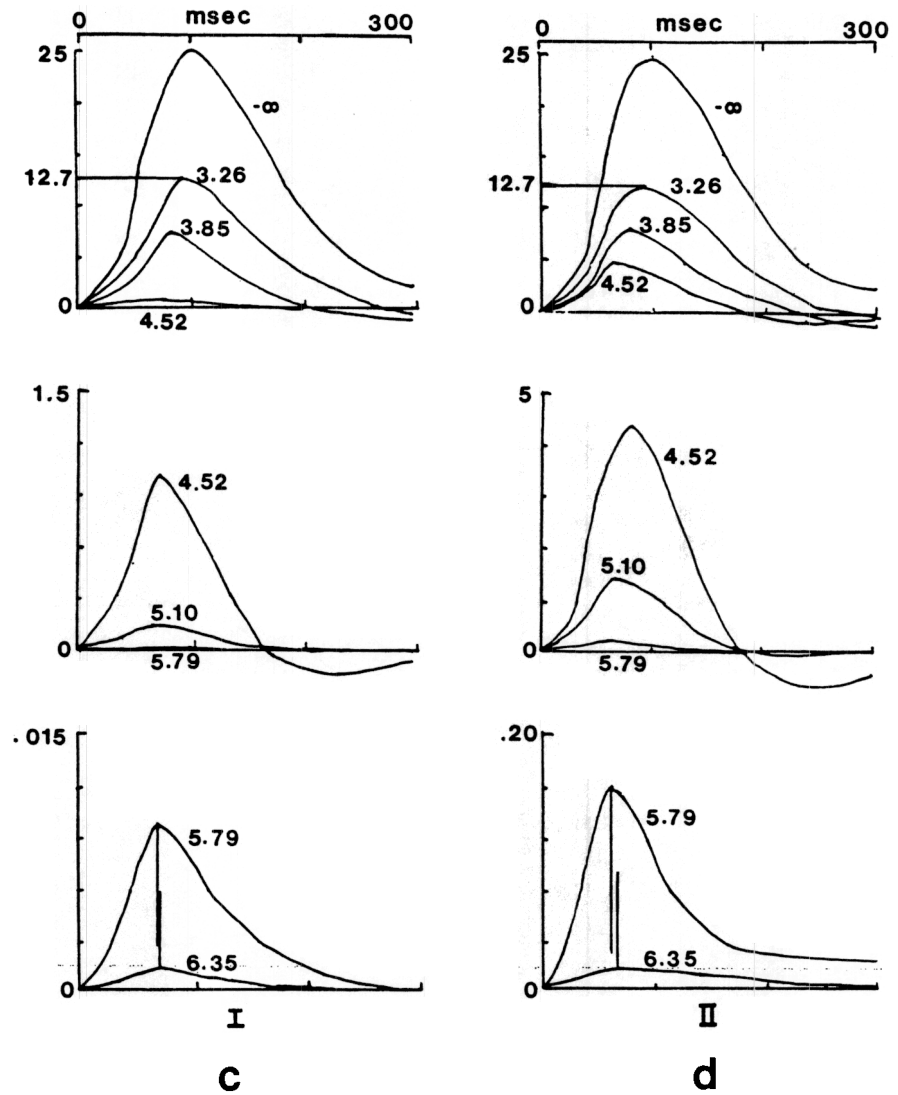


Fig. 14 (cont.). (c) Model I. (d) Model II. Note that the vertical scales are not all the same.

Figures 14–17 show that, of the three models under consideration, Model II provides the best fit to the data and BHL the poorest. Figure 14*a* presents the results of the intracellular recordings of Baylor and Hodgkin (1974); Figure 14*b* gives the predictions of BHL model; and Figures 14*c* and 14*d* give predictions of Models I and II. In each case, the peak potential in the dark is scaled to the value 25. The minimal background intensity is calibrated by finding that level at which the peak potential is 12.5, or half the peak in the dark. Thus each model fits the peak data exactly in the dark and with the lowest positive background intensity. Note that the vertical scale in Figure 14*d* (Model II) is the same as that of Figure 14*a*, which depicts the data. By contrast, the scales of Figure 14*b* (BHL) and Figure 14*c* (Model I) have been adjusted to accommodate the poorer match between the data and BHL and between the data and Model I. These results on peak potential are summarized in Figure 15.

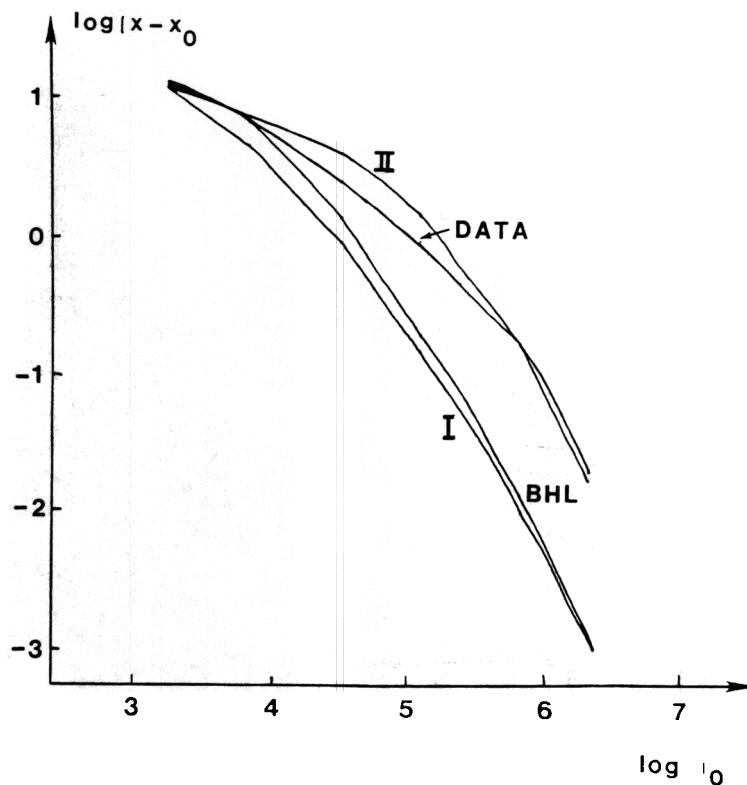


Fig. 15. The size of the peak hyperpolarization, as a function of  $\log_{10} I_0$ , for the Baylor–Hodgkin data and the three models. Note that at high input intensities, BHL differs from the data and Model II by a factor of 10.

Figure 16 indicates the time of peak hyperpolarization as a function of background intensity. Here, BHL gives a poor fit to the data; Model I gives a much better fit; and Model II, with the slow enzymatic activation, gives the best fit of all.

Figure 17 shows the fit of the steady-state data (equilibrium levels of  $x_0$ ) for the parameters chosen in each model.

#### The chain reaction

In Models I and II, the signal  $S(t)$  is given by a chain reaction described by Equation (84) (Baylor *et al.*, 1974a). The constants  $n$  and  $\gamma_1 \dots \gamma_n$  are chosen so that, when the light stimulus  $I(t)$  is a flash in the dark,  $S(t)$  matches the experimental dark response (top curve of Figure 14a). Since equation (84) is linear,  $S(t)$  is equal to the sum of the dark response curve plus a constant which is proportional to the background intensity. Consequently, in this paradigm, any choice of chain reaction constant which provides a good fit to the dark curve will fit the data as well as any other choice. A simple function form which provides an adequate fit in the dark is

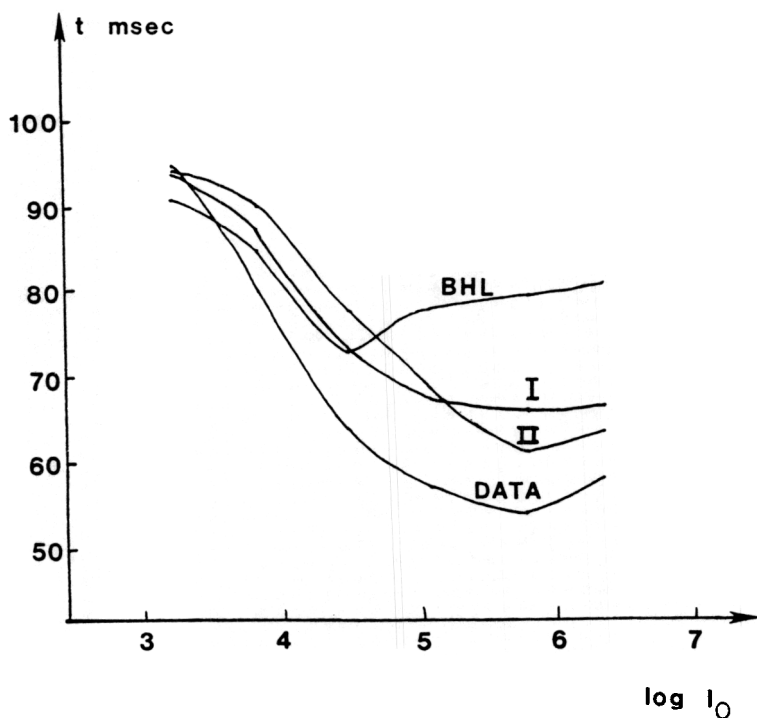


Fig. 16. Times at which the peak hyperpolarizations occur for the Baylor-Hodgkin data and the three models. Note that the input intensity at which the turn-around occurs and the dynamic range of peak times are much too small in the BHL model. BHL consider this the most serious defect of their model.

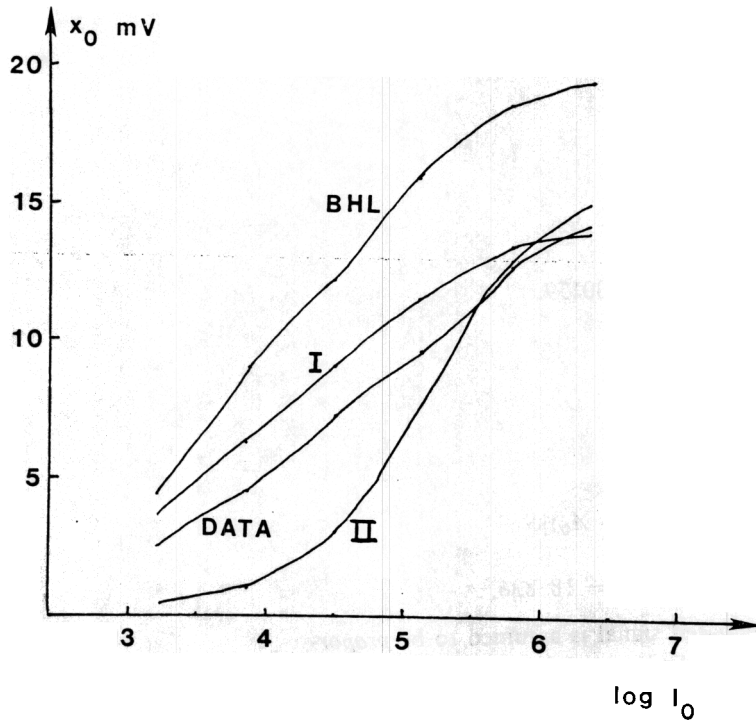


Fig. 17. Graphs of the steady-state hyperpolarization  $x_0$ , in response to the constant light intensity  $I_0$ , for the Baylor-Hodgkin data and the three models.

$$(86) \quad f(t) = J e^{-\gamma t} (1 - e^{-\gamma t})^5.$$

A suitable choice of constant  $J$  makes  $f(t)$  equal to  $S(t)$  in the dark when  $n = 6$  and

$$(87) \quad \gamma_1 = 6\gamma, \gamma_2 = 5\gamma, \dots, \gamma_6 = \gamma.$$

This is the 'independent activation' form of Baylor *et al.* (1974a). This form is used in Model I ( $\gamma = 17.3$ ) and Model II ( $\gamma = 17.6$ ). Other chain reactions give similar results.

In the BHL model, a similar chain reaction is used, except that the last step is modified to incorporate the unblocking variable  $z_2$  and the slow process  $z_3$  (Sections 13 and 15).

*Parameter values for Model I and Model II*

Equation (88) contains the parameter values chosen for Model I in Figures 14-17. Equation (89) contains the parameter values for Model II. We wish to

emphasize, however, that the model properties described in this section are robust over a wide range of parameter values and are not particular to the choices listed below.

*Model I*

$$(25) \quad \frac{dz}{dt} = A_0 \left[ \frac{1 + FS}{1 + GS} \right] (B - z) - Sz$$

$$(88) \quad A_0 = 1.8, F = 0.00333, G = 0.00179.$$

*Model II*

$$(4) \quad \frac{dz}{dt} = A(B - z) - Sz$$

$$(19) \quad \frac{dA}{dt} = -C(A - A_0) + D[E - (A - A_0)]S$$

$$(89) \quad A_0 = 0.5, C = 0.2, D = 0.00047, E = 18.836.$$

For each model,  $B$  is arbitrary, since the gated signal is assumed to be *proportional* to  $Sz$ : a particular  $B$  would just multiply  $Sz$  by a constant factor.

### 15. Comparison with the Baylor, Hodgkin, Lamb model

BHL first observed that the voltage response of a turtle cone to a weak and brief flash of light (e.g., 11 msec) can rise for over 100 milliseconds before it slowly decays over a period of several hundred milliseconds. In order to maintain a prolonged response after the flash terminates, they assume that light sets off a chain reaction (84). They also assume that, in response to small light signals, the change  $U(t)$  in membrane potential is proportional to  $y_n(t)$ .

The main physical idea is suggested by the fact that, in response to higher input intensities, the chain reaction fits the data during the rising portion of the potential, but yields higher values than the potential during its falling phase. Because this effect occurs at later times, it is ascribed to a process that is triggered at the end of the chain reaction. Because the potential undershoots the chain reaction, it is assumed that this late process interferes with the potential. Such considerations led BHL to argue that the chain reaction activates a process which elicits the initial hyperpolarization of the potential. Thus it is assumed that 'after a certain delay, light liberates a substance, possibly calcium ions, which blocks sodium channels in the outer segments' (Baylor *et al.*, 1974b, p. 760) and thereby tends to hyperpolarize the cone. The larger hyperpolarization produced by the chain reaction than the data is then ascribed to subsequent processes that interfere with ('unblock') the blocking substance during the falling phase of the potential. Their entire model is based on this assumption.

Denote the concentration of blocking substance by  $z_1(t)$  and the concentration of the unblocking substances by  $z_2(t)$  and  $z_3(t)$ . Function  $z_1(t)$  replaces the last stage  $y_n(t)$  of the chain reaction in (84). Baylor *et al.* (1974b) choose the equations for  $z_1$  to fit the data in Figure 3. To explain these and related data, it is assumed that the  $z_i$  act on each other via a nonlinear feedback process that is defined as follows:

$$(90) \quad \tau_L \dot{V} = E - V(1 + G_f + G_l)$$

$$(91) \quad G_l = \frac{G_l}{1 + \frac{z_1}{K}}$$

$$\tau_f \dot{G}_f = F(V) - G_f$$

$$(93) \quad F(V) = \frac{G_f}{1 + \exp [(V - V_f)/V_\epsilon]}$$

$$\left( \frac{d}{dt} + \alpha \right)^{n-1} y_{n-1} = \alpha^{n-2} I(t)$$

$$(95) \quad \dot{z}_1 = \alpha y_{n-1} - K_{12} z_1 + K_{21} z_2$$

$$(96) \quad \dot{z}_2 = K_{12} z_1 - (K_{21} + K_{23}) z_2 + K_{32} z_3$$

$$(97) \quad \dot{z}_3 = K_{23} z_2 - (K_{32} + K_{34}) z_3$$

$$(98) \quad AK_{21} = K_{12} = \bar{K}_{12} + v z_2 \left[ \frac{K_{12M} - \bar{K}_{12}}{K_{12M} - K_{12} + v z_2} \right].$$

Initial conditions on all  $y_i(t)$  and  $z_j(t)$  for  $t \leq 0$  are 0,  $V(0) = V_D$ , and  $V_D$ , the potential in darkness, satisfies

$$(99) \quad V_D \left[ 1 + \frac{G_f}{1 + \exp [(V_D - V_f)/V_\epsilon]} + G_l \right] = E$$

to make  $V_D$  an equilibrium point of (90) in the absence of light. The potential  $V$  is related to the hyperpolarization  $U$  via the equation  $U = V - V_D$ .

Equation (90) describes how the potential  $V$  is hyperpolarized by changes in the conductances  $G_f$  and  $G_l$ . Equation (91) shows that  $G_l$  is a decreasing function of  $z_1$ . Equations (92) and (93) say that  $G_f$  time-averages a logistic function of  $V$ . Equation (94) describes the chain reaction with end product  $y_{n-1}$  and light input  $I(t)$ . Equations (95)–(98) describe the nonlinear chain reaction of blocking and unblocking variables  $z_1$ ,  $z_2$  and  $z_3$  that is driven by the output  $y_{n-1}$  of the chain reaction. Equation (99) defines parameters to make  $V_D$  the equilibrium point of (90) when  $I(t) \equiv 0$ .

The Equations (90)–(99) are an ingenious interpretation of the data, but their

main features, such as the chain reaction of blocking and unblocking variables in (95)–(98), the non-linear dependence of the blocking and unblocking rates on these variables in (98), and the existence of the voltage-dependent conductance  $G_f$  in (92)–(93) are hard to interpret as logical consequences of a well-designed transducer, and have difficulties meeting the data quantitatively, as shown in Section 14.

To explain the turn-around of potential peaks, BHL use the nonlinear feedback process between blocking and unblocking variables in (90), (91), (95)–(98) to argue that ‘the shortening of the time to peak occurs because the concentration of  $z_2$  increases and speeds up the conversion of  $z_1$  to  $z_2$ ’ (Baylor *et al.* 1974*b*, p. 784). To explain the eventual slowdown of response to high background intensities, the parameters are chosen (e.g.,  $A > 1$  in (98)) so that ‘at very high levels of  $z_2$  the reaction is so fast that there is no initial peak and the reaction is in equilibrium throughout the whole response. This results in an increase in the time to peak because the rate of destruction of  $z_2$  at a high intensity is less than the rate of destruction of  $z_1$  at some lower intensity’ (Baylor *et al.* 1974*b*, p. 784). Thus, the existence of process  $z_2$  and its properties are postulated to fit these data rather than to satisfy fundamental design constraints. Of great qualitative importance is the fact that this explanation of the turn-around in potential peak implies the nonexistence of overshoots at high flash intensities. This implication does not hold in our gating model. It forces the following auxiliary hypotheses in the BHL model.

Baylor, Hodgkin and Lamb note that the above mechanisms do not suffice to explain certain phenomena that occur after a strong flash. In particular, the potential transiently overshoots its plateau, achieving a peak change of 15–25 mV, before it settles to a plateau of 12–20 mV. They did their double flash experiments (Figure 7) to study this phenomenon. In Figure 7, the second flash does not elicit a second overshoot, but rather merely prolongs the plateau phase. They need two variable conductances  $G_l$  and  $G_f$  to account for these data. The light-sensitive conductance  $G_l$  in (91) is a decreasing function of  $z_1$ , which is, in turn, an increasing function of light intensity due to (94) and (95). The conductance  $G_f$  in (92) depends on light only through changes in potential. In particular  $G_f$  is a time-average of a logistic function (93) of the potential. The main idea is that the light-sensitive conductance  $G_l$  is shut off by the first flash. This leads to an initial hyperpolarization which changes  $G_f$ . This latter change decreases the potential at which the cell saturates from 30 to 20 mV, and causes the potential to return towards its plateau value. At the plateau value,  $G_f$  is insensitive to a new flash, so a second overshoot does not occur, but the newly reactivated chain reaction does prolong the plateau phase.

Even without the extra conductance  $G_f$ , some overshoot can be achieved in the model in response to weaker lights which hyperpolarize  $U(t)$  by 5–10 mV. These overshoots are due to delayed desensitization, but they disappear when strong lights perturb the BHL model, unlike the situation in real cones; hence the need for  $G_f$ .

The authors also use the conductance  $G_f$  to explain why offset of a rectangular pulse of depolarizing current that is applied during a cone's response to light does cause a rebound hyperpolarization, whereas a depolarizing current in the absence of light does not (Figure 8).

## 16. Conclusion

We have indicated how a minimal model for a miniaturized unbiased transducer that is realized by a depletable chemical transmitter provides a conceptually simple and quantitatively accurate description of parametric turtle cone data. These improvements on the classical studies of Baylor, Hodgkin, and Lamb are, at bottom, due to the use of a 'gating' rather than an 'unblocking' concept to describe the transmitter's action. Having related the experiments on turtle cone to a general principle of neural design, we can recognize the great interest of testing whether analogous parametric experiments performed on nonvisual cells wherein slowly varying transmitters are suspected to act will also produce similar reactions in cell potential. Where the answer is 'no', can we attribute this fact to specialized differences in the enzymatic modulation of photoreceptor transmitters that enable them to cope with the wide dynamic range of light intensity fluctuations?

## References

- Arden, G. B. and Low, J. C. (1978). Changes in pigeon cone photocurrent caused by reduction in extracellular calcium activity. *J. Physiol.* **280**, 55–76.
- Bäckström, A.-C. and Hemilä, S. O. (1979). Dark-adaptation in frog rods: changes in the stimulus–response function. *J. Physiol.* **287**, 107–125.
- Baylor, D. A. and Hodgkin, A. L. (1974). Changes in time scale and sensitivity in turtle photoreceptors. *J. Physiol.* **242**, 729–758.
- Baylor, D. A., Hodgkin, A. L. and Lamb, T. D. (1974a). The electrical response of turtle cones to flashes and steps of light. *J. Physiol.* **242**, 685–727.
- Baylor, D. A., Hodgkin, A. L. and Lamb, T. D. (1974b). Reconstruction of the electrical responses of turtle cones to flashes and steps of light. *J. Physiol.* **242**, 759–791.
- Boynton, R. M. and Whitten, D. N. (1970). Visual adaptation in monkey cones: recordings of late receptor potentials. *Science* **170**, 1423–1426.
- Caldwell, P. C. (1971). Calcium movements in muscle. In: *Contractility of Muscle Cells and Related Processes* (Podolsky, R. J., Ed.), pp. 105–114. Prentice-Hall, Englewood Cliffs.
- Čapek, R., Esplin, D. W. and Salehmoghadam, S. (1971). Rates of transmitter turnover at the frog neuromuscular junction estimated by electrophysiological techniques. *J. Neurophysiol.* **34**, 831–841.
- Dowling, J. E. and Ripps, H. (1971). S-potentials in the skate retina. Intracellular recordings during light and dark adaptation. *J. Gen. Physiol.* **58**, 163–189.
- Dowling, J. E. and Ripps, H. (1972). Adaptation in skate photoreceptors. *J. Gen. Physiol.* **60**, 698–719.
- Eccles, J. C. (1964). *The Physiology of Synapses*. Springer-Verlag, New York.
- Esplin, D. W. and Zablocka-Esplin, B. (1971). Rates of transmitter turnover in spinal mono-synaptic pathway investigated by neurophysiological techniques. *J. Neurophysiol.* **34**, 842–859.

- Grabowski, S. R., Pinto, L. H. and Pak, W. L. (1972). Adaptation in retinal rods of axolotl: intracellular recordings. *Science* **176**, 1240-1243.
- Grossberg, S. (1968). Some physiological and biochemical consequences of psychological postulates. *Proc. Natl. Acad. Sci. U.S.A.* **60**, 758-765.
- Grossberg, S. (1969). On the production and release of chemical transmitters and related topics in cellular control. *J. Theor. Biol.* **22**, 325-364.
- Grossberg, S. (1972a). A neural theory of punishment and avoidance, I. Qualitative theory. *Math. Biosci.* **15**, 39-67.
- Grossberg, S. (1972b). A neural theory of punishment and avoidance, II. Quantitative theory. *Math. Biosci.* **15**, 253-285.
- Grossberg, S. (1975). A neural model of attention, reinforcement, and discrimination learning. *Int. Rev. Neurobiol.* **18**, 263-327.
- Grossberg, S. (1976). Adaptive pattern classification and universal recoding, II: Feedback, expectation, olfaction, and illusions. *Biol. Cybernetics* **23**, 187-202.
- Grossberg, S. (1978a). A theory of human memory: Self-organization and performance of sensory-motor codes, maps and plans. In: *Progress in Theoretical Biology* Vol 5 (Rosen, R. and Snell, F., Eds.) Academic Press, New York.
- Grossberg, S. (1978b). Behavioral contrast in short-term memory: Serial binary memory models or parallel continuous memory models? *J. Math. Psychol.* **17**, 199-219.
- Grossberg, S. (1980). How does a brain build a cognitive code? *Psychol. Rev.* **87**, 1-51.
- Grossberg, S. (1981a). Psychophysiological substrates of schedule interactions and behavioral contrast. In: *Mathematical Psychology and Psychophysiology* (Grossberg, S., Ed.). American Mathematical Society, Providence, R.I.
- Grossberg, S. (1981b). Some psychophysiological and pharmacological correlates of a developmental cognitive and motivational theory. In: *The Proceedings of the Sixth International Conference on Evoked Potentials* (Cohen, J., Karrer R. and Tueting, P., Eds.).
- Hemilä, S. (1977). Background adaptation in the rods of the frog's retina. *J. Physiol.* **265**, 721-741.
- Hemilä, S. (1978). An analysis of rod outer segment adaptation based on a simple equivalent circuit. *Biophys. Struct. Mechanism* **4**, 115-128.
- Kleinschmidt, J. (1973). Adaptation properties of intracellularly recorded gekko photoreceptor potentials. In: *Biochemistry and Physiology of Visual Pigments* (Langer, H., Ed.). Springer-Verlag, New York.
- Kleinschmidt, J. and Dowling, J. E. (1975). Intracellular recordings from gekko photoreceptors during light and dark adaptation. *J. Gen. Physiol.* **66**, 617-648.
- Norman, R. A. and Werblin, F. S. (1974). Control of retinal sensitivity, I: Light and dark adaptation of vertebrate rods and cones. *J. Gen. Physiol.* **63**, 37-61.
- Zablocka-Esplin, B. and Esplin, D. W. (1971). Persistent changes in transmission in spinal mono-synaptic pathway after prolonged tetanization. *J. Neurophysiol.* **34**, 860-867.